Parallel but distinct adaptive routes in the budding and fission yeasts after 10,000 generations of experimental evolution

Authors: Arnaud N'Guessan[1], Vivian Wang[1], Christopher W. Bakerlee[2,3,4], Jenya Belousova[2], Greta Brenna[2], Megan E. Dillingham[5], Thomas Dupic[2], Shreyas Gopalakrishnan[2], Juhee Goyal[2,6], Misha Gupta[2], Caroline Holmes[2], Parris T. Humphrey[2,4], Tanush Jagdish[2,4,5], Elizabeth R. Jerison[2,7,8], Milo S. Johnson[2,4], Katya Kosheleva[2,8], Katherine R. Lawrence[2,4,9], Jiseon Min[2,3,4,6], Alief Moulana[2], Shreyas V. Pai[2,5], Angela M. Phillips[2], Julia C. Piper[8,10], Ramya Purkanti[2,11], Artur Rego-Costa[2], Tatiana Ruiz-Bedoya[2], Cecilia Trivellin[2], Michael J. McDonald[2,12], Michael M. Desai[2,4,8], Alex N. Nguyen Ba[1,13]

1. Department of Cell and Systems Biology, University of Toronto, Ramsay Wright Laboratories, 25 Harbord St, M5S 3G5, Toronto, Ontario, Canada.
2. Department of Organismic and Evolutionary Biology, Harvard University, Cambridge MA 02138, USA
3. Department of Molecular and Cellular Biology, Harvard University, Cambridge, United States.
4. NSF-Simons Center for Mathematical and Statistical Analysis of Biology, Harvard University, Cambridge, United States.
5. Graduate Program in Systems, Synthetic, and Quantitative Biology, Harvard University, Cambridge, United States
6. John A Paulson School of Engineering and Applied Sciences, Harvard University, Cambridge, United States.
7. Department of Applied Physics, Stanford University, Stanford, United States.
8. Department of Physics, Harvard University, Cambridge MA 02138, USA
9. Department of Physics, Massachusetts Institute of Technology, Cambridge, United States.
10. AeroLabs, Aeronaut Brewing Co, Somerville, United States.
11. The Max Planck Institute of Molecular Cell Biology and Genetics, Dresden, Germany.
12. School of Biological Sciences, Monash University, Clayton, Victoria, Australia
13. Department of Biology, University of Toronto at Mississauga, 3359 Mississauga Rd, L5L 1C6, Mississauga, Ontario, Canada

ABSTRACT

Quantitative genetics approaches designed to understand the evolution of traits have helped improve our understanding of the genetic basis of adaptation. However, they often overlook crucial aspects of adaptation, including the long-term temporal evolutionary dynamics, the predictability of evolutionary outcomes, the influence of past evolution on future evolutionary trajectories (contingency), and the diversity of molecular mechanisms underlying adaptation. Experimental evolution has been a useful tool for answering these questions, but extracting fundamental principles and predictive features of evolutionary outcomes from these datasets remains challenging due to the large number of covariates and confounding effects, such as differences in experimental setup, species lifestyle, gene content, and evolution rate. Here, we sought to circumvent these challenges by comparing distant yeast species that share several

evolutionary features but differ mainly in evolutionary history and genome architecture, i.e. *Saccharomyces cerevisiae* and *Schizosaccharomyces pombe*. Thus, we evolved 10 populations of the fission yeast for 10,000 generations in the same conditions as a pre-existing budding yeast dataset (i.e. high-sugar media and hypoxic conditions), allowing us to observe repeatable evolutionary outcomes within species but diverse molecular mechanisms and targets of adaptation across species. The most frequent adapting route in these conditions involved upregulating fermentation genes and downregulating the glycolysis gene *pyk1*, which has not previously been observed in *S. cerevisiae* evolved populations or in wild *Kluyveromyces lactis,* but similar evolutionary paths have been observed in *Schizosaccharomyces japonicus* and in clinically relevant populations, such as some cancer cells. This suggests that parallelism is pervasive in the tree of life and that mechanisms of adaptation can be shared among closely related or distant species. Despite similar gene content and identical environments, recurrent adaptation across *S. pombe* populations involved different genes than in *S. cerevisiae* and was mostly detectable at the transcriptomic level. This suggests that trans-regulatory effects may play an important role in adaptation on short evolutionary timescales and that differences in evolutionary outcomes between these species may be attributed to contingency.

INTRODUCTION

Long-term experimental evolution has highlighted the predictability of high-level features of evolution like fitness trajectories[1–6]. While fitness gains follow a fairly reproducible pattern of declining adaptability, the exact mutations or the sequence in which they occur are typically unpredictable. Nevertheless, experimental evolution done in large replication with the budding yeast *Saccharomyces cerevisiae* has revealed extensive parallelism at the gene or pathway level[3,7,8], even across strains that differed by thousands of polymorphisms[9]. These general patterns of reproducibility during experimental evolution are also seen in different organisms. For instance, during the *Escherichia coli* Long-Term Experimental Evolution (LTEE), half of the populations evolved a mutator phenotype and quasi-stable lineage coexistence emerged in 75% of the populations[4]. Further, substantial parallelism at the gene level can also be observed throughout the 12 populations over (now greater than) 60,000 generations[4].

Unsurprisingly, the molecular targets of selection during these experiments differ substantially between *S. cerevisiae* and *E. coli*[3,6]. Likewise, comparing microbial laboratory evolution to experimental evolution done in *Caenorhabditis elegans* and *Drosophila melanogaster* does not reveal universal targets of adaptation[10,11]. Notwithstanding their vastly different gene content and cellular form, part of the reason for these differences in molecular adaptation is the different selection environments between experiments (the LTEE was done in DM25 minimal media, while yeast was done in YPD rich media or in synthetic dextrose complete media). However, another more interesting hypothesis for these differences relates to the role of evolutionary contingency in shaping the dynamics and targets of selection.

Contingency is the product of past evolution, whereby epistasis and genome structures can strongly influence future adaptive potential[1,12,13]. Thus, species can be constrained to alternative adaptive paths, leading to profoundly different molecular signatures of evolution. Contingency has been explored in the context of strains with different gene deletions[13–16] and has even been observed in experimental evolution. For instance, across the 12 *E. coli* populations evolving in the same conditions during the LTEE, one population developed the ability to grow aerobically on citrate, a rare phenotype in this species resulting from a rare genome rearrangement. This phenotype is far more readily evolvable within that population after this rearrangement[17]. Further, while half of the LTEE populations evolved a mutator phenotype, and 75% evolved stable lineage coexistence, these phenomena are not observed in *S. cerevisiae* laboratory evolution experiments in standard rich media or in minimal media, despite being entirely capable of achieving these through genetic engineering[18].

While studying evolution using very distinct organisms has provided important insights into general features of evolutionary dynamics, it has made it difficult to discern the effect of life history from other idiosyncrasies on the molecular targets of selection. Would we find the same targets of selection (genes), and a preference for the same molecular mechanisms if we had evolved a species with substantially similar gene contents to that of *E. coli* or *S. cerevisiae*? The difficulty in answering this question is also reinforced by the wide variety of mechanisms of rapid adaptation revealed by long-term evolution studies, e.g. hybridization, selection on standing variation, cross-feeding interactions, or phenotypic plasticity involving behavioral or transcriptomic changes[11].

Evaluating the impact of differences between such species on quantitative trait evolution could improve our understanding of the role of genetic architecture and life history in trait diversity.

One way to address how much these two factors might influence short- and long-term adaptation is through the yeast subphylum. Although it exhibits immense trait diversity and is as genetically diverse as the animal kingdom[19,20], species within have a comparable number of genes, and share many genes and metabolic pathways such that most species can grow in the same media. As an example, *Saccharomyces cerevisiae* and *Schizosaccharomyces pombe* share about 4,500 genes (out of approximately 6,000), but are so diverged that their genomes show no synteny[21,22]. Evolutionarily, they have similar spontaneous mutation rates and were both domesticated for their ability to ferment. Some notable differences are that *S. pombe* is naturally a haploid in the wild[23,24], while *S. cerevisiae* is usually found as a diploid[25,26]. This could affect the effectiveness of selection because mutations can be recessive in diploids. Therefore, the extant genome might have 'footprints' of this accumulated genetic load in *S. cerevisiae*[3,27]. Supporting this, heterosis has been observed in yeast from crosses of wild budding yeast strains[28,29]. Further, *S. cerevisiae* is within the clade of yeasts that have undergone the so-called 'whole-genome duplication event', which is thought to have profoundly shaped their metabolism due to functional divergence in paralogous gene copies[30]. Another major difference is that *S. pombe* cannot survive the loss of its mitochondrial DNA and relies on oxidative phosphorylation for growth, i.e. it is petite-negative, while *S. cerevisiae* can survive without mitochondrial DNA, i.e. it is petite-positive, highlighting a rare ability of budding yeast [31–33]. Thus, domestication, competition with other microorganisms, and exploration of poorly oxygenated niches might have led *S. cerevisiae* to produce and process ethanol more efficiently than *S. pombe* [34,35]. Therefore, their different life cycles and evolutionary histories could lead them to different evolutionary outcomes

Hints of the effects of contrasting life and evolutionary histories on evolutionary signatures emerge when comparing the molecular processes that are under selection and could potentially allow for the prediction of molecular evolution that may occur during experimental evolution. For example, *S. cerevisiae* gene content variation across strains is more frequent than in *S. pombe*, and loss-of-function (LOF) mutations, such as nonsense mutations and frameshift deletions, tend to be recurrently fixed across populations[36]. The rate of copy number variants (CNV) is also higher in the budding yeast sub-telomeric regions and can contribute to its adaptation[36]. Additionally, although *S. pombe* has a similar substitution rate to the budding yeast, it has a higher indel mutation rate with a bias toward insertions[37]. Previous genomic analyses also showed that 43% of *S. pombe* genes have introns compared to 5% in *S. cerevisiae* and upstream intergenic regions are larger in the former[38]. The difference in extent of non-coding regions is also present at the whole-genome level: annotated coding regions span around 70% of *S. cerevisiae* genome compared to 60% for *S. pombe*[39–41]. It is currently unknown if this implies that *S. pombe* would preferably adapt through regulatory changes while *S. cerevisiae* would do so through gene content changes and mutations in protein-coding genes. However, the mutations in the non-coding regions of *S. pombe* are known to be involved in transcription regulation and should affect trait evolution and adaptation[42]. Thus, comparing the evolutionary processes and targets of adaptation in *S. cerevisiae* and *S. pombe* through experimental evolution could help highlight factors explaining differences in evolutionary outcomes across and within species.

To address the gap in understanding how species with similar gene content, but different life histories, might evolve in the same environment, we undertook a laboratory evolution experiment where we founded about 16 populations, each of 5 different budding yeast species, as well as the *S. pombe* fission yeast. Here, we describe the dynamics and molecular evolution of the fission yeast populations over the first 10,000 generations. Fission yeast is considered the outgroup of this set of species, and so it serves as a useful anchor for expectations within our chosen fungal phylum. We analyze the mutational spectrum, the molecular evolutionary dynamics, and identify, through pathway enrichment analysis and whole transcriptome sequencing, a case of parallel evolution where *S. pombe* populations have rewired their central carbon metabolism to reduce dependency on oxygen, which mirrors similar events in wild *S. pombe* populations and in related *Schizosaccharomyces*[32,35,35,43,44].

RESULTS

Contrasting fitness gain of fission yeast during 10,000 generations of evolution

To compare the evolutionary processes contributing to adaptation and selection targets between *S. pombe* and *S. cerevisiae*, we founded 15 *S. pombe* populations and performed experimental evolution for 10,000 generations, collecting and freezing samples approximately every 70 generations in 27% glycerol (**Methods; Fig. 1**). The populations were all founded from single colonies of the same *S. pombe* haploid laboratory strain (972h-) and serially propagated in batch culture in one well of a lidded, unshaken flat-bottom 96-well plate in rich media at 30°C with a daily $1{:}2^{10}$ dilution. 5 populations were lost during the first 10,000 generations of evolution, due to contamination or mechanical pipetting errors. Because of the plate lidding and the absence of shaking, these conditions correspond to a high-sugar hypoxic environment. The media and temperature are also identical to our previous experimental evolution study, which analyzed 10,000 generations of evolution for *S. cerevisiae* populations that were passaged simultaneously using liquid handling robotics[3]. Although these growing conditions may be sub-optimal for growth of *S. pombe* and so the selection pressure faced by the species may differ, our experiment allows us to control for some of the environmental variate for the comparison of evolutionary outcome.

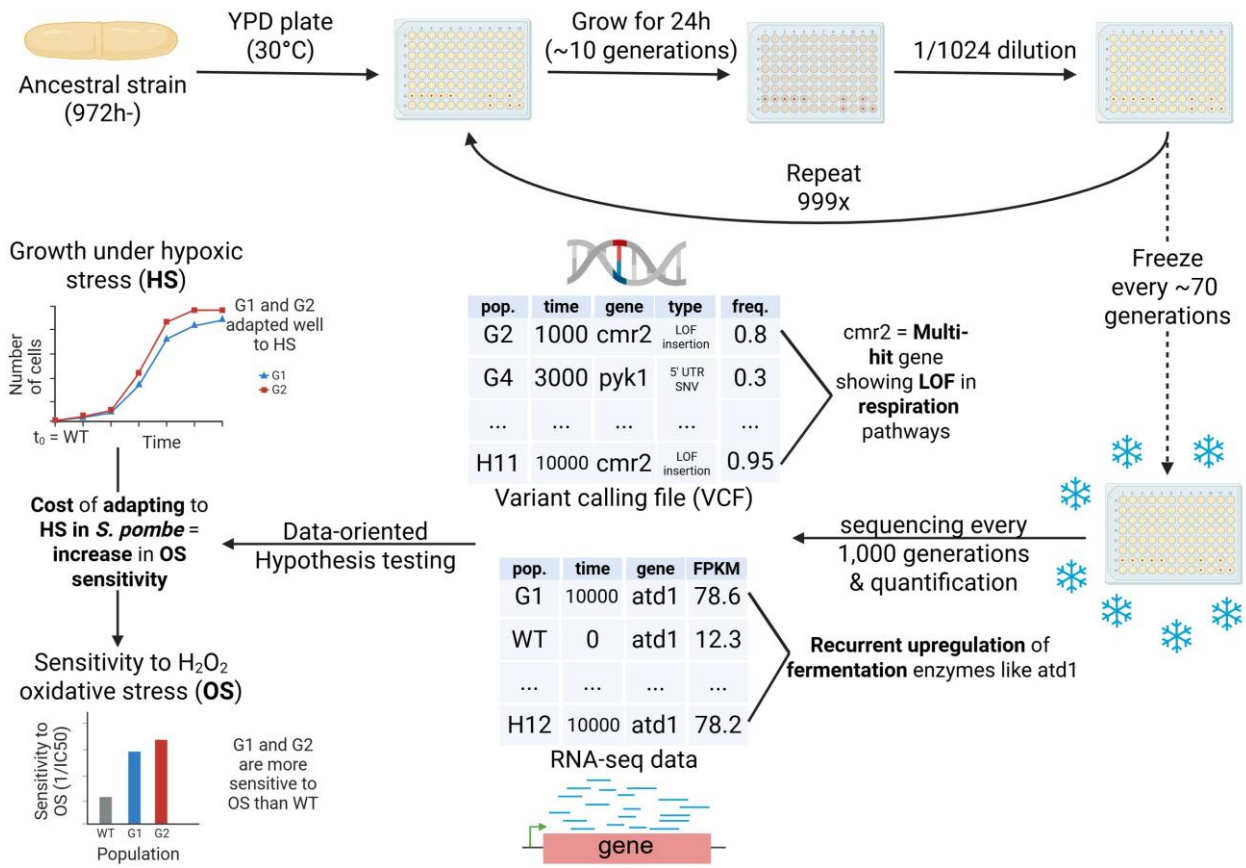

Figure 1 Experimental approach. We evolved 15 *S. pombe* populations at 30°C in lidded YPD 96-well plates for 10,000 generations, collecting and freezing samples approximately every 70 generations in 27% glycerol at -80 °C and sequenced them every 1,000 generations. These populations were part of a larger experimental evolution project, which explains why they occupy two rows of the 96-well plates and were examined regularly for contamination (**Methods**). Because the experimental conditions yielded a doubling rate of 10 generations per day, we performed a 1/1024 serial dilution every day ($1/2^{10}$), which can be done by two consecutive 1:32 dilutions with 96-well plates. This yielded ~100 time points or samples from which we sequenced DNA to identify variants. We also sequenced RNA at the initial (WT) and final time points to quantify gene expression changes. To find targets of selection at the genomic levels, we identified multi-hit genes, i.e. the genes that were recurrently hit by fixed mutations (frequency >= 75%) that are not synonymous (indels, missense, or nonsense) in multiple populations. At the transcriptomic level, we identified genes that were differentially expressed across several evolved populations compared to WT or to populations not exhibiting a change in a phenotype of interest, e.g. sensitivity to oxidative stress (OS). These data allowed us to generate hypotheses about adaptation in the 10 populations surviving, i.e. G1-G5, G9, H9 and H11-12, which we tested experimentally. For instance, in the figure, G1 (blue) and G2 (red) both adapts to hypoxic stress (HS) at the cost of becoming more sensitive to OS.

To determine whether the evolved populations adapted to these conditions, we measured the fitness at the initial and final time points. We serially propagated each population and the ancestral strain separately in a mixture with a *S. cerevisiae* reference strain expressing green

188 fluorescent protein (GFP) for 3 days. We used a flow cytometer to measure the frequency of the
189 dark *S. pombe* populations and the green *S. cerevisiae* strain daily, and assessed fitness based on
190 changes in frequency (**Equation 1 in Methods**). The evolved populations are all fitter than the
191 ancestral strain (**Supplementary Fig. 1**) as observed in other experimental evolution studies[3,6].
192 However, the fitness gains of the *S. pombe* lineages after 10,000 generations of evolution are
193 significantly smaller than those of *S. cerevisiae*'s haploid populations in a similar rich-media
194 hypoxic environment (**Supplementary Fig. 1**). This slower rate of fitness gain is not due to *S.*
195 *pombe* being 'pre-adapted' to this environment, as the ancestor *S. cerevisiae* strain used in a
196 previous study is much fitter than the ancestor *S. pombe* strain used here. We presume that this is
197 the result of *S. cerevisiae* having higher glycolytic and fermentation rates and being able to more
198 readily adapt to the experimental conditions through a more diverse set of stress response pathways
199 as a result of having explored many anaerobic niches throughout its evolutionary history[32,34,35,45].
200 *S. pombe*, on the other hand, is a poor fermenter in anaerobic conditions[32] and has a less robust
201 hypoxic stress response[46]. Together, these factors may partly explain differences in adaptation
202 rates under the same environmental conditions, as each species may evolve through different
203 adaptation strategies with different associated costs.

204

205 **Differences in the genome architecture partially explain the different mutation spectra of *S.***
206 ***pombe* and *S. cerevisiae***

207 To uncover potential differences in adaptation strategies between the two species and the
208 molecular mechanisms underlying them in the evolved populations, we performed whole-
209 population, whole-genome sequencing every 1,000 generations on the 10 *S. pombe* populations.
210 We successfully grew cells from 93 out of the 100 corresponding stored samples and sequenced
211 these time points using Illumina NovaSeq paired-end sequencing (mean coverage ~40X). The
212 remaining 7 time points were presumably lost during storage and were not associated to any
213 specific population or particular archival date. We then called single-nucleotide variants (SNVs)
214 and indels using Varscan2.4.6[47]. Because contamination, sequencing errors and low-complexity
215 regions can introduce variant calling errors, we applied some filters to the called variants [48,49] while
216 leveraging the time series for call consistency (**Methods**).

217 To validate the accuracy of the called variants, we measured the substitution rates and fixed
218 indel bias, e.g., the fixed insertion-to-deletion ratios, in each *S. pombe* population. We measured a
219 fixed insertion-to-deletion ratio ranging from 2.11 to 6.33 (median = 4.43, μ= 4.32, and σ= 1.22;
220 **Supplementary Fig. 2**), which is consistent with the insertion preference observed in previous *S.*
221 *pombe* genomic analyses [37]. As for the substitution rate, we measured an average of 1.91E-10 fixed
222 substitutions per site per generation (median = 1.72E-10, σ= 6.76E-11), which is similar to results
223 from mutation accumulation experiments in *S. pombe* (2.00E-10 in Farlow et al. 2015) and within
224 the range of *S. cerevisiae*'s substitution rate estimates (1.67 ± 0.04E-10 in Zhu et al. 2014 and
225 3.30± 0.80E-10 in Lynch et al. 2008)[37,50,51].

226 Although both species accumulate substitutions at a similar rate, their genome architectures
227 differ. *S. cerevisiae* is a domesticated post-WGD yeast species, contrary to *S. pombe* [52–55].

228 Furthermore, the extent of coding regions in *S. pombe*'s genome (~60%) is smaller than in *S.*
229 *cerevisiae* (~70%) [34,37,56,57]. Under a null model of evolution in which all loci have the same chance
230 of being hit by substitutions, the differences in the mutation spectra of these species should reflect
231 the differences in genome architecture. Deviations from this expectation would suggest the
232 presence of selection in certain loci and a preference for specific types of mutations. Thus, we
233 compared the frequency of different variants observed in the 10 *S. pombe* haploid populations to
234 the one observed in *S. cerevisiae* haploid populations' experimental evolution[3] (**Fig. 2A**).

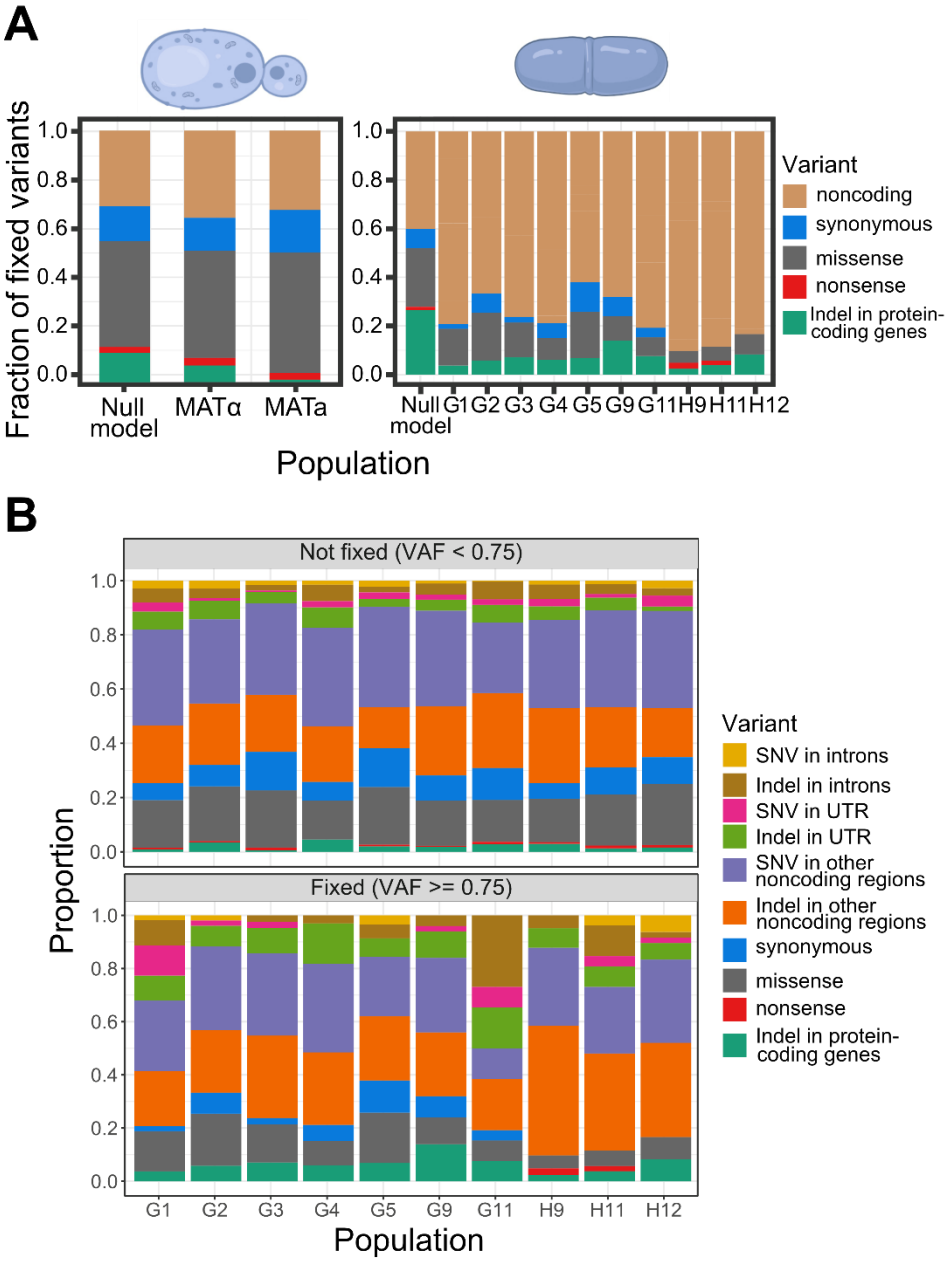

235 **Figure 2 Comparison of the fixed variant spectra between the budding and the fission yeasts**
236 **and the fixation bias in *S. pombe* evolved populations.** A) The fixed variant (allele frequency
237 >= 75%) spectrum in *S. cerevisiae*'s haploid populations after 10,000 generations of experimental

evolution (left, data from Johnson et al. 2021) compared to *S. pombe*'s (right). The experimental evolution protocol is the same for both species and is described in Johnson et al. 2021[3]. The null model is obtained by calculating the expected number of fixed variants in each category based on the species' evolution rate, genome size, genome architecture, and the proportion of single-nucleotide mutations derived from the genetic code and associated with a specific category of protein-coding region mutations (**Equations 2 and 3 in Methods**). B) The upper part of this panel represents non-fixed variants, while the bottom part represents the fixed variants in each of the 10 evolved *S. pombe* populations.

The fixation of variants in the noncoding regions of *S. pombe* is higher than expected by the null model, suggesting the predominance of positive selection in noncoding regions or purifying selection in coding regions. The fission yeast populations mainly evolved through mutations in non-coding regions with a bias toward fixing indels and not fixing coding regions SNVs (**Fig. 2B**), which is different than what has been reported for the budding yeast[3]. To test if the stronger fixation bias of indels in non-coding regions compared to protein-coding genes reflects a signal of purifying selection in protein-coding genes, we compared the indel rate, i.e., the number of indels per kb, based on whether the indel locus is coding or non-coding and whether the indel changes the DNA reading frame or not (**Supplementary Fig. 3**). In protein-coding genes, controlling for increased likelihood of shorter indels, we find that indels that do not cause frameshifts are enriched compared to the ones that do (**Supplementary Fig. 3**). In contrast, indels in non-coding regions do not exhibit such selective constraints on their length. This is similar to the observed frequencies of polymorphisms in humans and budding yeast[58] and suggests stronger purifying selection in protein-coding genes. This and the paucity of fixed coding mutations compared to *S. cerevisiae* populations suggest that the genetic context of *S. pombe* is less amenable to tinkering through loss-of-function mutations. One hypothesis for this may be that the whole-genome duplication event in *S. cerevisiae* provided more genetic redundancy, which has been suggested to increase evolvability through coding mutations or through rapid changes in functional gene content[30,59] (see Discussion). An additional explanation is that *S. pombe* has a much higher essential gene load than S. cerevisiae (26.1% vs 17.8%)[60]. Altogether, these results show that the differences in the mutation spectra of *S. cerevisiae* and *S. pombe* are only partially explained by their genome architectures, revealing signatures of selection in both coding and non-coding regions.

The genomic targets of adaptation in *S. pombe* are genes involved in the response to hypoxic and oxidative stresses

Although the *S. pombe* mutation spectrum revealed a signal of purifying selection in protein-coding genes, we cannot exclude the presence of loci evolving under positive selection. However, we may expect the targets of adaptation to vary between fission and budding yeasts due to differences in their evolutionary histories and genetic architectures. To detect such loci in 205 *S. cerevisiae* populations, Johnson et al. (2021) looked for signals of convergent evolution. More precisely, they defined a "hit" as a fixed variant that is not synonymous (missense, nonsense and indels), and a multi-hit gene as a gene having hits in multiple populations. This enabled the identification of 1,092 genes with hits in at least 3 out of 205 populations. Among these genes, they identified a set of 189 genes with hits in at least 6 populations that were enriched in functions

279 related to the adenine biosynthesis pathway, the mating pathway, and negative regulators of the
280 Ras pathway. These signals of parallelism at the levels of biosynthetic and signaling pathways
281 were driven by LOF mutations, which were primarily frameshift deletions and nonsense mutations.

282 Using the same approach with a minimum threshold of 2 out of 10 populations in which a
283 gene has a hit, we identified 19 multi-hit genes with hits in either the cis-regulatory region or the
284 coding region (**Table 1**). We note, however, that 10 indels were found repeatedly in many
285 populations (but not all). These may indicate remarkable genetic-level nucleotide convergence (or
286 rather strong mutational biases), or they may signal the presence of sequencing artifacts or
287 contamination. Upon inspection of these indels, we found that they were in homopolymeric tracts
288 and overwhelmingly had consistent allele frequency trajectories that, in isolation, would have
289 indicated a *bona fide* mutation (see **Methods** for details in how we characterize these). We thus
290 include them in our analyses but refrain from deriving any biological conclusions from these. If
291 they represent true mutational biases or signals of selection, we believe they warrant further study.

Gene symbol/ systematic ID (Number of populations with a hit (PH))	**Function(s) (biological process)**	**Gene category (Link with the response to HS and OS)**	**Characterization of the hit(s) (Gene product truncation or potential LOF)**
***bmc1*/ SPBC2A9.10** (2)	Bin3 family RNA methyltransferase (snRNA metabolic process)	Others	• 1 frameshift insertion in both G1 and G3 (Truncation of 14 out of 268 residues)
***bop1*/ SPAP32A8.03c** (2)	ubiquitin-protein ligase E3 (protein degradation)	HS-related (Ubiquitin-dependent protein degradation is ATP-dependent[61,62]. The response to HS requires specific E3 ligases that activate sterol regulatory elements (SRE) and the decrease of the activity of other E3 ligases that do not contribute to the HS response, e.g. Ubr1[63–65])	• 1 frameshift insertion in both G11 and H12 (Truncation of 475 out of 513 residues)

***clg1/* SPBC1D7.03** (2)	Cyclin-like protein involved in autophagy (signaling, molecular activity regulation and autophagy)	HS- and OS-related (in *S. pombe*, *clg1* regulates autophagy[66]. Autophagy plays an important role in the response to HS and OS by recycling biomolecules and removing damaged cell components[67,68])	• 1 indel in the 5'UTR of the populations G2 and G3
***cmr2/* SPAC56F8.02** (2)	acetyl-CoA biosynthesis (respiration)	HS- and OS-related (Acteyl-CoA is involved in the first step of the TCA cycle and respiration enzymes are involved in energy production and ROS removal[69])	• 1 missense mutation in the AMP-dependent synthetase/ligase domain[40] in G1 • 1 nonsense SNP in H11 (Truncation of 174 amino acid residues in the Dip2-like domain[40] out of 1517 protein residues)
***ctf18/* SPBC902.02c** (4)	Ctf18 RFC-like complex subunit Ctf18 (DNA replication)	HS-related (Upregulated under HS[67])	• 1 indel in the first intron of the gene in the populations G3, G5, H9, and H11
***dep1/* SPBC21C3.02c** (2)	Rpd3L histone deacetylase complex subunit (chromatin organization and transcription regulation)	HS-related (Upregulated under HS[67]. *dep1Δ* strain is more sensitive to hydrogen peroxide[70] than WT)	• 1 indel in 3'UTR in the populations G2 and G11
***fet4/* SPBP26C9.03c** (2)	plasma membrane iron/zinc ion transmembrane transporter	HS- and OS-related (Iron cofactors support major biochemical processes like	• 1 indel in 5'UTR in the populations G2 and H11

	(inorganic ion homeostasis and transmembrane transport)	the heme biosynthesis, TCA cycle, electron transport chain, translation, and DNA repair[71])	
***fhn1/* SPBC1685.13** (3)	Eisosome assembly protein (membrane organization)	HS-related (Upregulated during the response to hydrogen peroxide[72])	• 1 indel in 3'UTR in the populations G3 and H11. 1 indel in 3'UTR in the populations G9
***iss9/* SPBC2A9.11c** (2)	SAC3/GANP/THP3 family protein (transcription or RNA surveillance)	Others	• 1 frameshift insertion in the populations G1 and G5 (Truncation of 315 out of 395 residues)
***pfl2* SPAPB15E9.01c** (3)	cell surface glycoprotein, flocculin Pfl2 (cell adhesion)	HS- and OS-related (Flocculation and adhesion enhance survival by protecting against stressful conditions[73,74])	• 5 missense hits in G3: chrI_A3989282G (R->G), chrI_G3989285A (A->T), chrI_G3989294A (G->S), chrI_G3989384A (G->S), chrI_G3989390A (A->T) 4 missense hits in G5: chrI_G3989877C (R->T), chrI_G3989879A (G->R), chrI_A3989878T (R->S), chrI_G3989877C (R->T) *Pfl2 is a disordered protein so it has many S, R and T residues[40,75] • 2 indels in 5'UTR in the populations G1 and G5
***pfl5/* SPBC1289.15** (3)	cell surface glycoprotein**,** flocculin Pfl5 (cell adhesion)	HS- and OS-related (Flocculation and adhesion enhance survival by protecting against stressful conditions[73,74])	• 2 Y→F missense hits in G2 and H12 around the middle of the protein. 1 K→E missense hit in G5 • The same frameshift insertion in the populations G2 and H12 (Truncation of 518 out of 1283 residues around the middle of the protein). 1 deletion in G2 (Truncation of 528 out of

			1283 residues around the middle of the protein)
***pof15/* SPAPB1A10.14** (2)	Ubiquitin complex adaptor; F-box protein (protein degradation)	HS-related (Downregulated under HS[67,76]. Ubiquitin-dependent protein degradation is ATP-dependent [61,62])	• 1 N→D missense hit in G5 • 1 frameshift deletion in the population H12 (Truncation of 135 out of 243 residues)
***pqr1/* SPAC6B12.07c** (3)	SPX-RING-type ubiquitin-protein ligase regulating phosphate transport and homeostasis (protein degradation and transmembrane transport)	HS-related (Upregulated during the response to hydrogen peroxide[72]. Excess of intracellular phosphate and polyphosphate is associated with improper autophagy-dependent proteolysis in vacuoles[77])	• 1 SNV in 3'UTR in G9, G11 and H11
***prr1/* SPAC8C9.14** (2)	stress-responsive DNA-binding transcription factor Prr1 (transcription regulation and response to oxidative stress)	OS-related (*prr1* is a positive regulator of the OS response. It binds *pap1* as part of a positive regulation of transcription, and it regulates *ctt1*, *srx1*, *trr1* during the cellular response to OS[78,79])	• 1 P→Q missense hit in the signal transduction response regulator/receiver domain in H12 • 1 frameshift insertion in the population H11 (Truncation of 517 out of 540 residues)
***pyk1/* SPAC4H3.10c** (5)	pyruvate kinase (carbohydrate metabolic process)	HS- and OS-related (The gene product catalyzes the last step of glycolysis. This	• 1 missense hit V→L in the barrel domain in H11 • 2 SNVs in 3' UTR in G1 • 1 SNV in 3' UTR in H12 • 1 deletion in the promoter (5' UTR) in G3

		influences the fermentation-respiration balance and thus biomass production and stress resistance[35])	• 1 deletion in 5' UTR in G4
***pzh1/* SPAC57A7.08** (2)	serine/threonine protein phosphatase (signaling)	HS- and OS-related (*pzh1* is a positive regulator of the response to OS[80]. It is also upregulated under HS[67])	• 1 deletion of 2 residues (positions 73 and 74) in the N-terminal disordered region[40] in both G5 and G9
***rpp1/* SPAC3A12.04c** (2)	RNase P and RNase MRP subunit p30 (ribosome biogenesis and tRNA metabolic process)	Others	• 1 SNV in the fourth intron of the gene in populations H11 and H12
***seb1/* SPAC222.09** (2)	poly(A)site selection protein (mRNA metabolic process and snoRNA metabolic process)	Others	• 1 missense T→I hit in the RNA recognition motif domain in G1 • 1 missense K→N hit in the CTD-interacting domain in G2
***ubp9/* SPBC1703.12** (2)	ubiquitin C-terminal hydrolase Ubp9 (protein degradation and vesicle-mediated transport)	HS- and OS-related (*ubp9Δ* strain is more sensitive to hydrogen peroxide[70]. Protein degradation and vesicle-mediated transport enable the recycling of biomolecules under stress conditions[61,62])	• 1 frameshift insertion in the populations G3 and G9 (Truncation of 265 out of 585 residues, including most of the ubiquitin carboxyl-terminal hydrolase domain)

292 **Table 1 Multi-hit genes and their LOF mutations.** The gene annotations are based on Pombase
293 data[40].

294 The presence of hits in multi-hit genes was more recurrent than expected under a null model where
295 variants are fixed at the same rate across all the genes (**Methods**; Two-sided Wilcoxon rank sum
296 p-value < 0.05; **Supplementary Fig. 4**). This signal of positive selection is also consistent with
297 the fixation of these hits (**Fig. 3**) and the fixation of the same hit at different times in multiple
298 populations (**Table 1**; **Fig. 3**), though we note some of multi-hit genes may be due to mutational
299 biases.

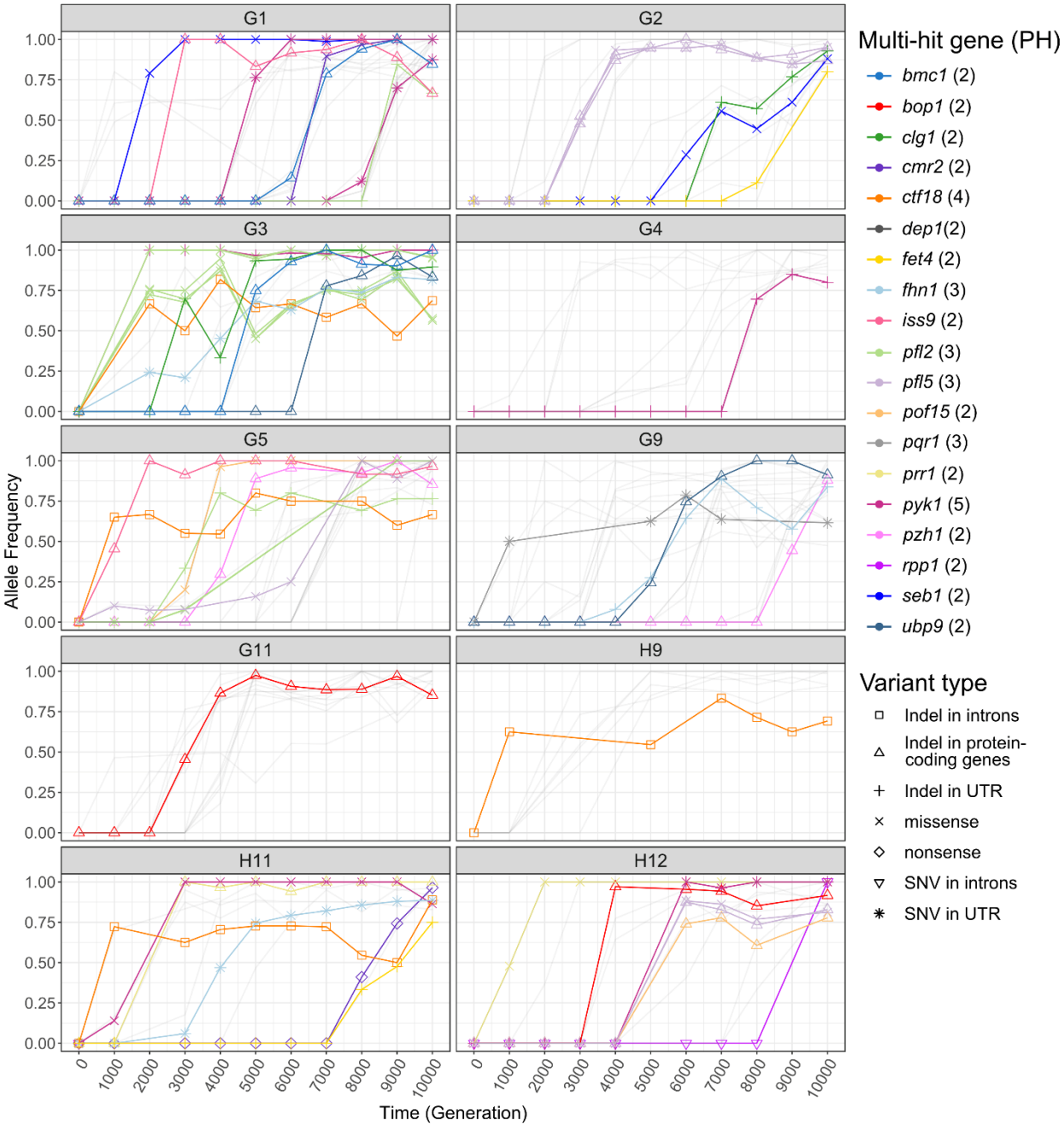

Figure 3 Time series of the hits' allele frequencies in evolved *S. pombe* populations and multi-hit genes. Time series of the hits' allele frequencies in the *S. pombe* populations. We defined a "hit" as a fixed genic variant that is not synonymous (missense, nonsense and indels) and a multi-hit gene as a gene having hits in multiple populations. In each population, variants that were never fixed or that are not located in multi-hit genes are represented by more transparent lines. In the legend, PH represents the number of populations in which the gene is hit.

We also found evidence for adaptation through LOF mutations in the 10 evolved *S. pombe* populations, although these mutations are primarily frameshift insertions rather than deletions.

308 This is consistent with a different indel bias than in *S. cerevisiae*[3] (**Table 1; Fig. 2**) and a preference
309 for insertion, which we previously highlighted (**Supplementary Fig. 2**).

310 Most of the *S. pombe* multi-hit genes are involved in the response to hypoxic stress (HS)
311 and sometimes to oxidative stress (OS) (**Table 1**), which may be due to growth in an unshaken
312 and lidded environment. Adapting to HS requires compensating for the energy deficit caused by
313 respiration deficiency through fermentation and removing the associated reactive oxygen species
314 (ROS)[32]. Further, the increase in ethanol or acetate production through fermentation can hinder
315 mitochondrial membrane integrity and functions, leading to ROS production[45,81–85]. This is
316 consistent with fixed mutations in genes involved in the removal of damaged cell components and
317 ROS like *clg1*, *pqr1*, *pzh1* and *ubp9*. Fermentation is also known to yield smaller energy and
318 biomass outputs than respiration [32,34], which can affect the synthesis of redox metabolism
319 components. Finally, *S. pombe* is known to be sensitive to polypeptones included in the growth
320 media of the experiment (due to cell lysis), and it is thought that the respiratory Coenzyme Q
321 (CoQ10) plays a role in promoting this trait[86,87]. Under the same conditions, *S. cerevisiae*, being
322 petite-positive, can rely on fermentation along with a robust antioxidant response to mitigate the
323 ROS produced by fermentation and hypoxic stress[45], which may explain why such mutations are
324 not typically observed in budding yeast experimental evolution studies.

325 Another piece of evidence supporting the importance of energy- and ROS-related processes
326 in this environment is the fact that the strongest signal of convergent evolution is in the lower
327 glycolysis gene *pyk1*, which had fixed mutations in 5 populations. This gene encodes for the
328 enzyme involved in the synthesis of pyruvate, which influences respiration and fermentation as it
329 can be transformed into Acetyl-CoA or into acetate and ethanol, the fermentation products[35]. In
330 the population H11, the glycolytic flux going towards respiration seems to be compromised by a
331 fixed LOF mutation in *cmr2* (**Fig. 3**), which encodes for the enzyme converting pyruvate into
332 Acetyl-CoA. The fixation of this LOF mutation might be related to a benefit in re-orienting the
333 glycolytic flux mostly towards fermentation. In the same population, we also observed the fixation
334 of a LOF mutation in *prr1*, which encodes a transcription factor involved in the response to OS.
335 Because *prr1* is not known to be directly activated by HS, there might be other OS response genes
336 involved in ROS removal under HS, and *prr1* might not be needed unless ROS levels exceed the
337 removal capabilities of these genes. For instance, in *S. pombe,* the transcription factor Sre1 is
338 activated under low oxygen levels and activates genes involved in ROS removal or protein
339 catabolism like *ccs1* and *SPAC23C11.06c*[67,88]. The benefit of inactivating *prr1* while respiration
340 is limited under HS might thus be related to conserving energy and cell resources. However, losing
341 such response regulators and relying on fermentation may make *S. pombe* more sensitive to OS.

342 **Most evolved *S. pombe* populations are more sensitive to oxidative stress**

343 As we observed fixed LOF mutations in genes modulating OS response and the glycolytic flux
344 towards respiration, we hypothesized that evolved populations might be more sensitive to OS.
345 Populations adapting to hypoxic stress or to polypeptone-mediated lysis may exhibit decreased
346 respiration rates, resulting in reduced energy and biomass production[32]. This could affect the
347 synthesis of the components of the redox metabolism, e.g. glutathione (GSH) and ubiquinone
348 (CoQ10)[69,89]. These enzymes and the ones involved in the respiratory chain rely on the biomass

349 produced by glycolysis and the TCA cycle as well as ions like iron and sulfur for their
350 functions[32,89–91]. Consistent with this, we observed the presence of hits in the iron transporter *fet4*
351 in multiple populations, which may compensate for respiration deficiency. Indeed, iron can help
352 capture or transport the low amount of oxygen available, and iron is a critical component of the
353 respiratory chain enzymes. Moreover, one *S. pombe* evolved population harbors a LOF insertion
354 in *prr1* (**Table1**, **Fig. 3**), an important transcription factor involved in the response to oxidative
355 stress[79]. As *prr1* activates the catalase *ctt1*, the sulfiredoxin *srx1*, and the thioredoxin *trr1*[78], a fixed
356 LOF mutation in this gene suggests that evolving under HS can decrease *S. pombe*'s ability to
357 manage OS, which is consistent with observations in the cousin species *S. japonicus*[32]. These
358 species likely rely on fermentation to adapt to hypoxic conditions, which may expose them to more
359 ROS[45]. Altogether, these observations led us to believe that the evolved *S. pombe* populations are
360 more sensitive to OS than WT as a result of their adaptation to HS.

361 To test this, we used hydrogen peroxide as a source of oxidative stress during a growth
362 assay (**Methods**) and compared the OS sensitivity of the WT to the OS sensitivity of the 10 evolved
363 populations (**Fig. 4A**).

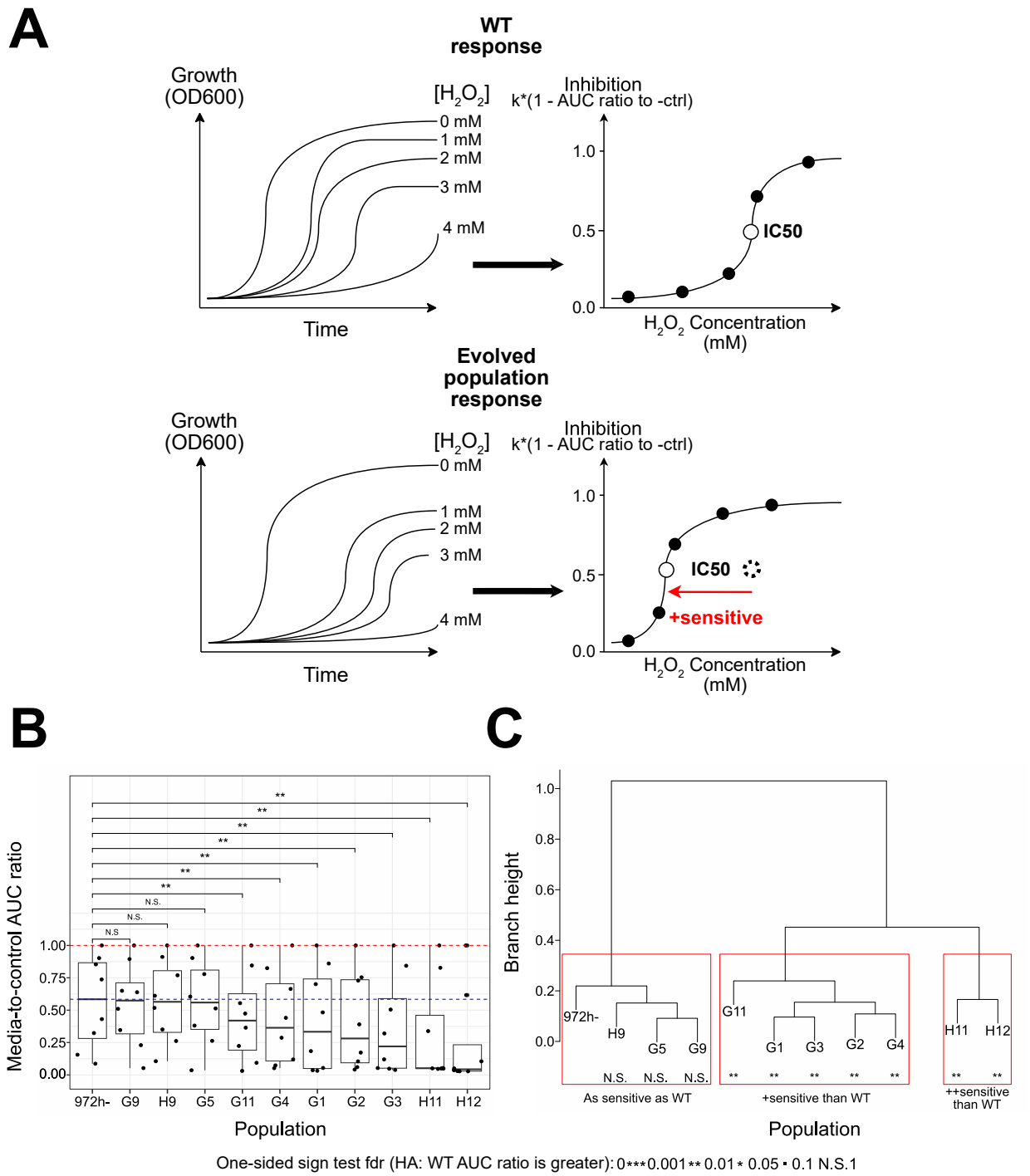

Figure 4 Comparison of the sensitivity levels to H_2O_2 between *S. pombe* WT and evolved populations. A) Schematic illustrating the expected difference in sensitivity between WT and evolved populations. We inferred the degree of inhibition at each concentration of H_2O_2 based on the expression in Equation 4 and the sensitivity of each population based on Dose-Response analysis (**Methods**). The IC50 recapitulates the level of sensitivity of a population to hydrogen peroxide. Lower IC50 values can be interpreted as higher sensitivity to H_2O_2, which is what we expected for the evolved populations. B) The ratio between the AUC of a population at a certain

371 H_2O_2 concentration + YPD and the AUC in YPD without H_2O_2. Each point is a different
372 concentration. This is another metric of sensitivity with an expected maximum of 1 (red dotted
373 line). The blue dotted line represents the median sensitivity of the WT. The WT AUC ratio is
374 compared to each evolved population using a sign test on the ranks. The one-sided adjusted p-
375 values (false discovery rates; alternative hypothesis="WT AUC ratio is greater than evolved
376 populations'") of this test are encoded as follows: *** from 0 to 0.001 exclusively, ** from 0.001
377 to 0.01 exclusively, * from 0.01 to 0.05 exclusively, "." from 0.05 to 0.1 exclusively and N.S.
378 otherwise, which is the acronym of "non-significant". C) Red boxes represent the population
379 clusters, which are based on the AUC ratios.

380 The evolved populations clustered into 3 groups: 3 out of 10 populations had a similar sensitivity
381 to H_2O_2 as the WT, 5 out of 10 populations were more sensitive than WT, and 2 out of 10 evolved
382 populations were much more sensitive than the WT strain, including H11, the population that lost
383 the OS response regulator *prr1* (**Fig. 4B** and **4C**). This increased sensitivity to OS after adapting
384 to HS has not been observed in *S. cerevisiae*, which may be explained by contingency, i.e. more
385 exposure to anaerobic environments during its evolutionary history and a better redox
386 metabolism[32,34]. However, it is reproducible in most of the evolved *S. pombe* populations, and has
387 likewise been observed in related species, including wild *S. japonicus*[32] (see Discussion).

388 **Transcriptomics analysis reveals many genes involved in the response to HS and downstream**
389 **effects explaining the sensitivity to OS in multiple populations**

390 The sensitivity to OS developed after adapting to HS was revealed by convergent evolution at the
391 genomic level, i.e. multi-hit genes. However, identifying transcriptomic differences between more
392 sensitive and WT-like populations could help reveal genes driving this evolutionary outcome and
393 explain how point mutations and indels contribute to the evolution of these traits through
394 transcriptomic regulation. Moreover, most of the mutations in the pyruvate kinase (*pyk1*) locus are
395 located in the untranslated regions flanking the gene, which contains cis-regulatory elements
396 (CRE) like the promoter (**Supplementary Fig. 5**). Hits in these loci could explain the adaptation
397 to HS through changes in transcript levels through cis-regulatory and trans-regulatory effects[92–96].
398 These questions thus led us to investigate the role of transcriptomic changes in the responses to
399 HS and OS. To do so, we performed RNA-seq of the WT ancestor and the final evolved
400 populations, and compared the transcriptomic profiles of populations more sensitive to H_2O_2 than
401 WT with those of populations as sensitive as WT (**Methods**).

402 Consistent with the need to compensate for biomass and energy deficit under HS due to
403 limited respiration[32], most evolved *S. pombe* populations upregulated genes involved in heme
404 metabolism/transport, the transport of biomolecules like amino acids or hexose, lipid metabolism,
405 fermentation, and ion transport (**Fig. 5, Supplementary Table 1**).

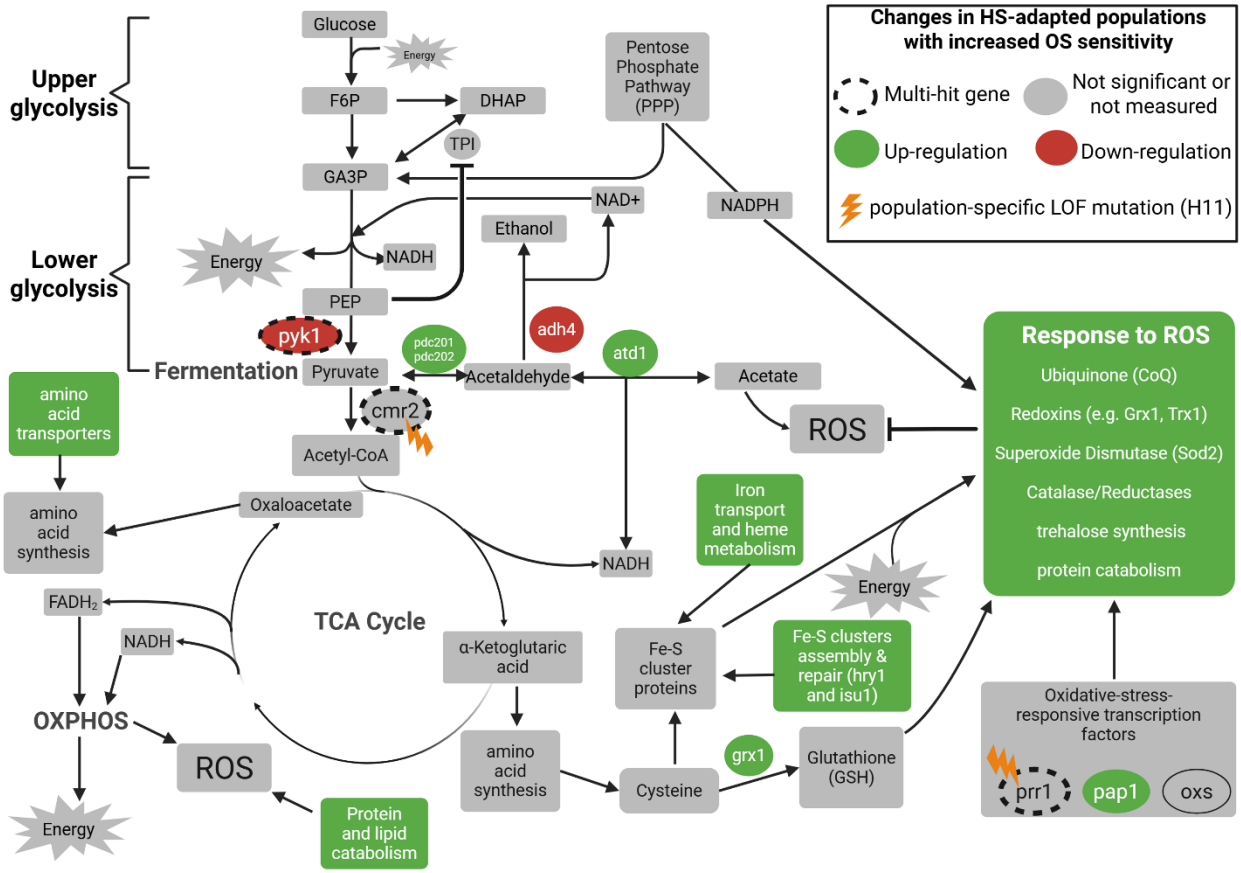

Figure 5 Fission yeast cellular responses to hypoxic stress in populations with increased OS sensitivity. Transcriptomic changes are determined by comparing the populations with increased OS sensitivity to populations with similar OS sensitivity than WT while genomic changes are obtained by comparing these evolved populations to WT (**Methods**). The green fill represents an upregulation while the red fill represents a downregulation. When processes are color filled, they represent cases where some genes involved in those processes were upregulated. The grey fill represents molecules or processes that were not associated with a gene with significant effect or not measured (no data). The orange lightning symbol represents LOF hits in H11, the only population with such variants in several multi-hit genes (dotted line stroke).

Another way the fission yeast populations could respond to HS is by improving the electron transport chain (ETC) to leverage the limited amount of oxygen available. The upregulation of the heme transporters *str3* and *shu1* in many evolved populations supports such a strategy (**Supplementary Table 1**). Heme can help capture and transport the small amount of oxygen available under HS and it is an essential component of the electron transport chain (ETC)[90].

Despite the presence of transcriptomic changes explaining HS adaptation and the OS sensitivity cost, most of the differentially expressed genes were different than the targets of selection identified at the genomic level, except for *pyk1*, *pzh1* and *ubp9*. For instance, the multi-hit gene *clg1*, which is a positive regulator of autophagy[40,66], is not differentially expressed between populations with different OS sensitivity, but 22 other genes involved in autophagy exhibit an expression level increase from 54.4% to 229% (**Supplementary Table 1**) and they are

426 not mutated. Autophagy might be one of the few pathways that contribute to cross-resistance to
427 both HS and OS by recycling biomolecules and removing damaged cell components[67,68]. This is
428 consistent with the upregulation of the multi-hit gene *pqr1*, the ubiquitin-protein ligase regulating
429 phosphate transport and homeostasis, such that autophagy is not compromised in vacuoles[77].
430 Another process linked to cross-resistance to multiple stresses is vesicular transport[97,98]. One of its
431 genes, i.e. *ubp9,* is one of the only three multi-hit genes to be differentially expressed in evolved
432 *S. pombe* populations that are more sensitive to OS than WT (log2FC = 0.867; FDR<0.05),
433 suggesting a moderate but significant link between vesicular transport and adaptation
434 (**Supplementary Table 1)**. As for the multi-hit gene *pyk1*, it is downregulated by 36.5% in
435 populations with increased OS sensitivity (FDR<0.05; **Supplementary Fig. 6**). Adaptation to HS
436 may require decreasing the glycolytic flux allocated to respiration[32] and change the
437 respiration/fermentation balance. This is consistent with the decrease of Acetyl-CoA synthesis
438 through the downregulation of the Acetyl-CoA ligase *pcs60* (53.7% decrease; FDR<0.05) and
439 selected LOF mutations in *cmr2*, which may trigger the ETC optimization responses previously
440 described as a compensatory mechanism. Similar to mutations observed in *S. japonicus*, the LOF
441 mutations in lower glycolysis and Acetyl-CoA synthesis might also contribute to OS sensitivity in
442 *S. pombe* as it would decrease the biomass and energy output of respiration, which is used for the
443 synthesis of redox metabolism proteins[69,89]. The last differentially expressed multi-hit gene is *pzh1*
444 (log2FC = 0.752; FDR<0.05), which regulates the activity of the plasma membrane H+-ATPase[99].
445 This is consistent with the need to increase energy production to compensate for respiration
446 deficiency in hypoxic conditions.

447 Apart from these three multi-hit genes, transcriptomic changes shared by populations with
448 increased OS sensitivity involved genes that were not mutated at the genomic level
449 (**Supplementary Table 1; Table 1**). This is the case for many upregulated genes involved in
450 fermentation, e.g. *pdc201/202* and *atd1*, and in the synthesis of ETC components and their iron-
451 sulfur clusters, e.g. *cbp3-4, cbp6, coq9, sdh3, sdh8*, *qcr7-10*, *fxn1* and *isu1*. The lack of overlap
452 between selection targets at the genomic and transcriptomic levels suggests that the overall
453 changes in expression levels shared by many evolved populations are driven by trans-regulatory
454 rather than by cis-regulatory effects. However, interpreting metabolic fluxes from transcriptomics
455 data remains challenging and further exploration into the mechanisms affected by this rewiring is
456 needed to reveal more deeply how they relate to adaptation in our environment.

457 **DISCUSSION**

458 Over short periods of time, experimental evolution is a powerful tool to decipher molecular
459 pathways under selective constraints[3,11]. An important result from studies exploiting asexual
460 laboratory evolution is that evolution is usually not limited by mutation: adaptation usually
461 proceeds rapidly and is often dominated by large-effect mutations. In many cases, gene content
462 variation can occur (via ploidy changes), and mutations frequently inactivate gene function.
463 Perhaps the most interesting result from many of these studies is that laboratory evolution can
464 frequently recapitulate evolutionary outcomes from wild, uncontrolled evolution. Whole-genome
465 duplication, loss-of-function mutations, the rise of mutators, stable co-existence, and like here the
466 change of carbon flow towards increased fermentation, are all phenomena thought to have
467 occurred in various species at various times during their evolutionary history, but also notably in
468 cancer cells[11,100–102]. The fact that cancer cells are also evolving populations suggests that
469 experimental evolution in different single-cell organisms can reveal fundamental principles of the

470 molecular basis of adaptation. For instance, the pervasiveness of parallel evolution in the tree of
471 life could be explained by deep conservation of interconnected biological pathways.

472 Our study extends the discovery of shared molecular mechanisms of adaptation across scales in
473 diverse biological systems. For instance, *S. pombe* shares a distinct preference for insertions as a
474 mutational bias with *C. elegans*[38,]. On specific selection targets, mutations that lead to upregulation
475 of iron metabolism, autophagy regulators and vesicle transporters, and that lead to rewiring of the
476 glycolytic flux are common observations in populations adapting under iron and oxygen
477 limitation[104,105] (such as tumors). The fact that the orthologs *pykF* and *pyk1* in *E. coli* and *S. pombe*,
478 respectively, are both recurrently hit across multiple populations illustrates the conservation of
479 some selection targets at the gene level, even across distant species. Finally, parallel evolution
480 within model systems is frequent and has been observed in nearly all experimental evolution
481 studies to date, but the precise observed trait under selection varies (examples in [6,106] and reviewed
482 in[107]).

483 Despite all these common evolutionary mechanisms and outcomes, disparities can arise
484 due to differences in genome architecture and contingency. One of the major findings in
485 evolutionary dynamics is that low-fitness populations typically adapt faster than high-fitness
486 populations. This observation has been seen in several species, and in several environmental
487 contexts[3,6,11]. In the evolution environment of our study, the 'ancestor' *S. cerevisiae* is much fitter
488 than its *S. pombe* counterpart. Yet, the fitness gains by our *S. pombe* populations are relatively
489 modest (**Supplementary Fig. 1**). We propose that one explanation for this 'evolvability' is the
490 effect that we set out to study in the first place, which is evolutionary contingency. Indeed, in a
491 previous study, it was found that the identity of specific molecular pathways of gene deletions had
492 a strong impact on fitness gain after evolution[13].

493 Further supporting this, the most frequent targets of adaptation in the past *S. cerevisiae*
494 study were genes involved in adenine biosynthesis and the mating pathway, for which genomic
495 hits have high fitness effects[3]. However, these pathways are not targets of selection in these *S.*
496 *pombe* populations. Based on our understanding of the adenine biosynthetic pathways in both
497 species, mutations in adenine biosynthesis genes were not expected in our *S. pombe* populations
498 (which are ade+). In contrast, the *S. cerevisiae* populations were *ade2*-, which led them to
499 accumulate a toxic intermediate that can be suppressed by the observed adenine pathway mutations
500 after evolution. It is well known that similar effects can be observed in *ade6*- strains of *S. pombe*[108].
501 Similarly, mutations in the mating pathway might not be observed in *S. pombe* due to its
502 preferential haploid lifestyle and its mating pathway is not active in rich media[23,24].

503 A third pathway frequently mutated in the budding yeast laboratory evolution experiment
504 is the Ras-cAMP pathway[3,8,109]. Observed loss-of-function mutations in *IRA1* or *IRA2* (but usually
505 not both), relieve inhibition of Ras and lead to PKA activation [3,110]. Activation of PKA ultimately
506 leads to increased glycolysis through phosphorylation of Pyk1[111]. Our *S. pombe* populations never
507 mutated the *IRA1/2* ortholog (*gap1*), though we note that it is a single-copy gene in the fission
508 yeast. More surprisingly though, are the mutations observed in *pyk1*. These mutations are not the
509 usual loss-of-function nonsense or frameshift mutations. Instead, most mutations were found in
510 the regulatory region of the gene, which we initially believed to be an analogous way for *S. pombe*

511 to upregulate Pyk1 activity. However, whole-transcriptome analyses suggest that these mutations
512 downregulate Pyk1 activity (**Fig. 5**). Interestingly, similar mutations leading to lower Pyk1 activity
513 have been observed in wild *S. pombe* populations and in the common laboratory strain[35],
514 suggesting that decreasing Pyk1 activity may be adaptive. In Kamrad et al. (2020), the authors
515 showed that a decrease in Pyk1 activity does not increase growth rate nor biomass, seemingly
516 contradicting the strong signature of adaptation from parallel evolution. However, the authors
517 noted that lower Pyk1 activity might be an adaptive trade-off as lower glycolytic flux increases
518 oxidative stress resistance through higher pentose-phosphate pathway flux and NADPH
519 production. Despite transcriptomic analyses showing a slight decrease in *pyk1* expression levels in
520 most evolved *S. pombe* populations, they were often more sensitive to OS than WT. This is
521 potentially explained by the fact that during our experiment, the slightly reduced glycolytic flux is
522 mostly redirected toward fermentation, which is upregulated to compensate for the fission yeast
523 respiration deficiency in hypoxic conditions.

524 Adaptation to our growth environment has led to an increased OS sensitivity for most
525 evolved populations via multiple molecular mechanisms. First, Pyk1 activity can regulate carbon
526 flow and, like the other mutations found in the wild, can favor fermentation rather than respiration,
527 as our lidded and unshaking environment is likely to lead to hypoxic stress. Supporting this, we
528 observed adaptations to HS, including LOF in enzymes responsible for the transition between
529 glycolysis and oxidative phosphorylation, and the upregulation of the fermentation rate. This leads
530 to an increase in intracellular ROS through higher ethanol production and a deficiency in the
531 production of biomass and energy, which sustains the redox metabolism[34,45]. In our dataset, 3
532 populations in which *pyk1* is downregulated have cis-regulatory mutations around the gene, while
533 G2 is the only population in which *pyk1* is downregulated without such mutations
534 (**Supplementary Figs. 5 and 6)**. This suggests that *pyk1* downregulation can evolve more easily
535 through cis-regulatory effects, but it can also evolve through trans-regulatory effects. The effect
536 of reducing Pyk1 activity here is also consistent with the other mutations we observed that appear
537 to modulate central carbon metabolism (**Figs. 3 and 5**). Second, *S. pombe* cells are sensitive to
538 polypeptones, a major component of our environment[86]. Mutations that lower respiration and flux
539 through the mitochondrial electron transport chain have been shown to increase resistance to
540 polypeptones because this sensitivity requires CoQ10[86]. Strikingly, there is also evidence in *S.*
541 *japonicus* that lower glycolysis is frequently being rewired in natural populations[32]. This suggests
542 that adaptation to HS or polypeptones in petite-negative yeast species with relatively modest
543 fermentation rates might often come at the expense of costly carbon flow rewiring, hindering the
544 response to OS.

545 Multiple genomic variants and transcriptomic changes were involved in the apparent trade-
546 off between HS and OS, e.g. the LOF or downregulation of some genes in lower glycolysis or
547 Acetyl-CoA synthesis, the upregulation of genes in fermentation, and the upregulation of genes in
548 the transport and metabolism of biomolecules and ions. Among these adaptations to HS,
549 fermentation upregulation and LOF in lower glycolysis and genes involved in the response to
550 oxidative stress such as *prr1*, may explain the increased sensitivity to OS. However, some genes
551 involved in OS response, autophagy and vesicle transport may contribute to cross-resistance to
552 both stresses[97,98,112–114] and indeed we observed three populations (G5, G9, and H9) with hits in

553 those pathways that did not appear to have increased OS sensitivity and those populations retain
554 WT-like expression level of the lower glycolysis pathway. This cross-resistance is also observed
555 in other species like *K. lactis, S. cerevisiae*, and human cancer[115–118]. In *S. pombe*, the effect of the
556 cross-resistance pathways was at times insufficient to offset the cost of adapting to HS by rewiring
557 of the glycolytic flux toward fermentation and using it as the main source of biomass and energy.
558 The fact that this trade-off has not been observed in the budding yeast may be explained by its
559 historical exposure to multiple anaerobic environments and more optimal adaptations to HS[34]. In
560 contrast, *S. pombe* and *S. japonicus,* for which lower glycolysis is less active compared to *S.*
561 *cerevisiae*, tend to adapt to HS through LOF in lower glycolysis and upregulation of fermentation
562 and upper glycolysis[32,35]. Furthermore, the fact that the response to HS mostly involved
563 transcriptomic changes in genes that were not mutated in coding or flanking regulatory regions
564 suggests that the adaptive transcriptomic changes observed across populations were driven by
565 trans-regulatory rather than cis-regulatory effects. This also shows that the transcriptome, an
566 intermediate level of organization between genotype and phenotype, is a complex trait that can
567 exhibit evolutionary parallelism.

568 Despite the potential of these observations to improve evolutionary predictions, this study
569 shows that multiple mechanisms are involved and that contingency can lead to diverse
570 evolutionary outcomes, even within a single species and under the same conditions. One way that
571 future research could better predict adaptive trajectories under stress conditions is by leveraging
572 the presence of rapid transcriptomic changes in response to a new stress independently of
573 mutations, e.g. expression plasticity. These responses could provide hints toward adaptive cellular
574 changes that could later be cemented by mutations with similar effects, as is the case in bird species
575 that explore high-altitude conditions[11,119].

576 **METHODS**

577 **Experimental evolution and sequencing**

578 We evolved 15 *S. pombe* populations of the laboratory strain 972h- at 30 °C in wells of a lidded,
579 flat-bottom 96-well plate containing 128 µl of YPD plus antibiotics (1% yeast extract, 2% peptone,
580 2% dextrose, 100 µg/mL ampicillin, 25 µg/mL tetracycline) for 10,000 generations, collecting and
581 freezing samples at -80 °C every 70 generations. The remaining wells contained blank controls or
582 populations of other yeast species and will be described elsewhere. This is the same procedure
583 used to generate the compared *S. cerevisiae* dataset[3]. Because these conditions yield a doubling
584 rate of 10 generations per day, we performed a 1/1024 serial dilution every day ($1/2^{10}$). This
585 corresponds to an effective population size of ~6.00E04 and a bottleneck population size of
586 ~8.00E03 [3,120]. We chose to perform whole-population whole-genome sequencing every 1,000
587 generations, and we were able to grow back cells from 93 out of these 100 samples after storage
588 and sequenced these time points with Illumina NovaSeq paired-end sequencing (mean effective
589 coverage ~40X). Sequencing and DNA preparation was performed as in the *S. cerevisiae* dataset.
590 Raw DNA sequences are available on NCBI:
591 https://www.ncbi.nlm.nih.gov/bioproject/PRJNA1315931.

592

593 **Measuring fitness in the *S. pombe* populations**

594 We grew the evolved populations, the WT, and a *S. cerevisiae* reference strain expressing GFP
595 (YAN438: *MAT*α *his3*Δ1 *ura3*Δ0 *leu2*Δ0 *lys2*Δ0 *can1*::*RPL39pr-ymGFP_STE2pr-*
596 *SpHIS5_STE3pr-LEU2*), for 24 hours. In contrast to our previous study[3], this *S. cerevisiae* strain
597 does not express a killer phenotype as it does not possess ScV-M1 killer-virus RNA. Next, because
598 the green *S. cerevisiae* strain grew much faster than *S. pombe,* we prepared mixtures of the "dark"
599 *S. pombe* populations and the green budding yeast at a 9:1 ratio and grew the mixed cultures for
600 24 hours. This ratio also reduces potential species interactions between *S. cerevisiae* and *S. pombe*.
601 We then serially propagated each mixture for 3 days and used a Beckman-Coulter CytoFlex flow
602 cytometer to measure the frequency of the "dark" *S. pombe* and the green *S. cerevisiae* strain daily.
603 All particle counts were acquired at 30 µL/s rate for a maximum of 60 seconds or until 10,000
604 events were detected from a 96-well plate containing the mixtures. The data were analyzed using
605 the CytoFlex acquisition and analysis software CytExpert. The "dark" *S. pombe* cells were
606 distinguished from the green *S. cerevisiae* strain using FITC-A/PE-A gates. This process was
607 replicated on a different day for biological replicates. Using the cell counts, we then calculated the
608 frequency of each population in the mixture and inferred fitness based on the slope of a linear
609 regression between the logarithm of the frequency ratio and the number of generations:

610 $$\ln\left(\frac{frequency_{S.\ pombe}}{frequency_{green\ S.\ cerevisiae}}\right) = (Fitness * number\ of\ generations) + intercept \qquad \text{(Eq. 1)}$$

611

612 The final fitness was the average of the two biological replicates.

613 **Variant calling**

614 We used Varscan2.4.6[47] to call single-nucleotide variants (SNVs) and indels. Because
615 contamination, sequencing errors and low-complexity regions can affect the variant calling, we
616 applied some filters to the called variants (Table 2). These filters ensure that the calls are supported
617 by reads, are time-consistent, and are not affected by possible errors in the reference genome, e.g.
618 avoiding confusion between ancestral alleles that were not present in the reference genome (972h-
619) and fixed de novo mutations. Briefly, the filters used mapping and read base quality, allele
620 frequency and absence of strand biases. In addition, because of the relatively sparse sequencing of
621 our experiment (every 1000 generations), most genuine mutations will be fixed in cohorts or
622 throughout the experiment, we also employed a filter for genetic hitchhiking and clonality.

623 When applying these filters, we also found 10 cases where the same recurrent indel in low-
624 complexity region was called in multiple populations. While these can be signatures of strong
625 mutation bias or strong selection, they can also indicate evidence of cross-contamination in the
626 evolution or DNA sequencing, as well as mis-indexed reads or read mapping issues. To rule these
627 out, we applied several manual inspections. First, when mutations arise in a population and fix,
628 they must remain fixed for the rest of the evolution. Second, if a recurrent mutation fixes in two
629 populations, they must not substantially share other mutations within the samples and the rest of
630 the time course (which would indicate cross-contamination). And third, other populations must
631 not show strong evidence of these mutations (which would indicate some sequencing bias). While

632 this does not rule out all possible issues with long-term evolution experiment and robotic
633 passaging, or other artifacts of our variant calling pipeline, these mutations were still considered
634 in our analyses as they may reveal mutational biases or other interesting phenomena (such as
635 genetic-level nucleotide convergence). Despite these filters, three variants remain ambiguous (in
636 *dep1, rpp1, pqr1*). A version of **Fig. 3** without these recurrent mutations is found in
637 **Supplementary Fig. 7**.

638 We also found cases of mutations that appeared to remain at intermediate frequencies, one of which
639 was recurrent (e.g. *ctf18*). This could indicate some form of frequency dependence or aneuploidy,
640 but it can also be a signature of a read mapping artifact. To explore this, we manually inspected
641 the mapped reads and found that these occurred in large polynucleotide tracts. As reads may not
642 always span the whole tract, variant calling algorithms may fail to capture indels as fixed. We
643 decided to leave the estimated frequencies as is.

644 Finally, complex mutations, such as events that may replace several adjacent codons
645 simultaneously, may be due to alternative read mapping locations or due to complex short-tract
646 recombination. We used the mapping quality filter to remove cases of alternative read mapping
647 locations, and thus these complex mutations were left as is by the variant calling pipeline as they
648 may be genuinely multiple mutations in the same region that get fixed. Nevertheless, this means
649 that some categories of mutations may be inflated due to incorporation from a complex event.

650 The variant calling pipeline is available at
651 https://github.com/arnaud00013/Experimental_evolution_S_pombe.

Filter name	Criteria
Mapping quality	Mapping quality score ≥ 15
Indels in low-complexity regions (short tandem repeats or homopolymers)	-Systematically eliminate the ones that are not supported by multiple timepoints -For the recurrent ones, because they could reveal a signal of selection, they were manually investigated in IGV to make sure there are no mapping mistakes, and multiple reads in both strands should support them. We also ensured that they were not introduced or fixed at the same time across multiple populations or systematically with the same group of alleles (**Fig. 3**), which could indicate contamination.
Read bases quality	≥ Q20
Allele frequency	≥ 0.05
Coverage and supporting reads	Coverage ≥ 5 and at least one read in both strands support the variant (so at least 2 supporting reads in total, and always 2 supporting strands)
Contamination	Because the *S. pombe* populations were grown in parallel with populations from other

	yeast species (*C. glabrata* CBS138, *K. lactis* NRRL-Y-1140, *P. pastoris* EAMORG09, *S. cerevisiae* YJM978, *S. paradoxus* IFO1804; **Fig. 1**), we made sure that the reads we recovered from sequencing best map to *S. pombe*
Evidence for sub-clonality and linkage disequilibrium	|Pearson r| ≥ 0.9 with at least one mutation from the same population
Variation in non-fixed variant allele frequency	≥ 0.1
Initial allele frequency	Eliminate variants with an allele frequency ≥ 0.4 in at least a third of the populations

Table 2 List of variant calling filters.

Identifying signatures of selection from the substitution spectrum

We defined substitutions as variants with an allele frequency >= 75%. Then, we compared the substitution spectrum of each population with the one expected after 10,000 generations of evolution under a neutral null model. The number of fixed variants in each mutation category is calculated based on the species' evolution rate, genome size, genome architecture (e.g. ratio of coding to non-coding regions in the genome), and the proportion of single-nucleotide mutations derived from the genetic code and associated with a specific category of mutations. This allowed to derive 2 equations:

$$Nb_subs_in_category_X_nm = S_{rate} * t * G_{size} * r_x * p_x \quad \text{(Eq. 2)}$$

$$Nb_indels_in_category_X_nm = I_{rate} * t * G_{size} * r_x \quad \text{(Eq. 3)}$$

where $Nb_subs_in_category_X_nm$ is the expected number of substitutions in a mutation category X assuming a neutral model of evolution, $Nb_indels_in_category_X_nm$ is the expected number of indels of type X assuming a neutral model of evolution, S_{rate} is the species substitution rate, I_{rate} is the species indel rate, t is the number of generations observed since the start of the experiment, G_{size} is the species genome size, r_x is the proportion of the genome covered by protein-coding or non-coding sites, depending on the mutation category X and p_x is the proportion of single-nucleotide mutations derived from the genetic code that can be classified as mutations from category X.

Next, we sought signatures of parallelism and positive selection in protein-coding genes among the fixed variants. We defined a "hit" as a fixed variant that is not synonymous (missense, nonsense, or indel), and a multi-hit gene as a gene with hits in multiple populations. (in at least 2 out of 10 populations). We then compared the number of population hits (PH) in the set of multi-hit genes to the PH expected under a null model, assuming that all genes evolve and fix variants at the same rate. The expected PH was determined based on a number drawn from a Poisson distribution where the argument λ (average number of events per interval) is the product of S.

679 pombe's substitution rate, the gene length, the generation time, the number of populations, and the
680 proportion of fixed variants that are not synonymous as determined in equations 2 and 3.

681 **Evaluating and comparing the sensitivity to hydrogen peroxide**

682 We grew the 10 evolved *S. pombe* populations and the WT ancestor in the rows of a 96-well plate
683 at 30°C for 36 hours. The media was YPD + hydrogen peroxide with H_2O_2 concentrations of 0
684 mM, 0.5 mM, 1 mM, 1.5 mM, 2 mM, 2.5 mM, 3 mM and 3.5 mM. Each row of the 96-well plate
685 corresponded to a different concentration of H_2O_2. The growth of each population was estimated
686 using the OD600 time series measured from a BioTek Synergy HTX plate reader. For each time
687 series, the area under the curve (AUC) was measured using the R package package
688 growthcurver[121]. Using the AUC as a proxy for growth, we then compared the AUC of each
689 population at different H_2O_2 concentrations to the AUC obtained when H_2O_2 is absent from the
690 media. Next, we inferred the degree of inhibition with:

691 $$Inhibition = k * \frac{AUC_{media}}{AUC_{control}} \quad \text{(Eq. 4)}$$

692 where k is a normalizing factor that makes sure the inhibition metric maximum is 1, AUC is the
693 area under the growth curve, AUC_{media} represents the growth at a certain concentration of
694 hydrogen peroxide and $AUC_{control}$ represents the growth in a YPD media without hydrogen
695 peroxide. This expression is negatively correlated to the AUC ratio and ranges from 0 to 1. Using
696 the Dose-Response Analysis R package drc[122], we then fitted a log-logistic model to this metric
697 and H_2O_2 concentrations to estimate the IC50, which recapitulates the level of sensitivity of a
698 population to hydrogen peroxide. Data in the manuscript is a representative result of the less noisy
699 biological replicate as determined by curve fit. Additionally, we found that the hydrogen peroxide
700 concentration tended to vary due to instability of the chemical, which would at times shift the
701 IC50, without changing the interpretation of the experiment. Finally, we performed a cluster
702 analysis on the populations based on their distribution of AUC media-to-control ratio at different
703 concentrations. We used the hclust function from the package stats v4.1.2[123] to perform the
704 clustering and the composition of each cluster was identical no matter the distance metric tested
705 (Gower, Manhattan, Euclidean, Bray-Curtis), which we obtained with the function vegdist from
706 the package vegan 2.7-2[124]. Growth curve figures are also shown in **Supplementary Fig. 8**.

707 **RNA extraction, sequencing and transcriptomic analysis**

708 We extracted in two biological replicates the RNA of the evolved populations using an in-house
709 protocol that works well with *S. cerevisiae*. Briefly, cells were grown to mid-log phase in YPD by
710 diluted overnight saturated cultures and growing for 4-6 hours and lysed using 100 µl of 5 mg/mL
711 Zymolyase + 10 mM DTT, incubated at 37 °Celsius for 5 minutes. The weakened cells were then
712 incubated with 100 µl of 2% SDS for a final SDS concentration of 1%. 200 µl of lysis buffer was
713 added (4.5 M Guanidine thiocyanate, 10 mM EDTA) and mixed gently by inverting. Lysate
714 clarification indicated complete lysis. The SDS was then precipitated using 200 µl of 3M
715 Potassium acetate at pH 5.

716 After centrifugation, the lysate was passed through a minipreparation silica column to bind DNA.
717 Under these conditions, RNA does not bind to the silica columns. Therefore, we collected the

718 flowthrough. We then mixed it with an equal volume of pure isopropanol and passed it through
719 another minipreparation silica column (which will now bind RNA). The column was then washed
720 with 400 µl of wash buffer (10% Guanidine thiocyanate, 25% Isopropanol, and 10 mM EDTA),
721 and then twice with 600 µl of 80% Ethanol. After drying the column, the RNA was eluted with 50
722 µl of 10 mM Tris pH 8.5. RNA integrity was verified on an agarose gel. One population (H12)
723 failed to get sufficiently high-quality RNA for sequencing.

724 We sequenced the successfully extracted RNA using NEBNext Ultra II on an Illumina NovaSeq
725 X paired-end sequencing lane. This yielded 10.6E06 150-bp paired-end reads per sample on
726 average (σ=1.32E06). Raw RNA-sequencing data are available on NCBI:
727 https://www.ncbi.nlm.nih.gov/bioproject/PRJNA1315931. We pre-processed the reads with fastp
728 (version 0.23.1) with the arguments --trim_poly_x --trim_poly_g --cut_front --
729 cut_front_mean_quality 20 --cut_tail --cut_tail_mean_quality 20 --detect_adapter_for_pe[125].
730 Next, we mapped the reads to the reference (972h-) using samtools v1.17, removed duplicates with
731 picard v2.26.3 and counted the number of reads per gene using featureCounts from subread
732 v2.0.6[126–128], and the counts were converted to FPKM. We then performed PCA analysis of the
733 transcriptome and found two main clusters (PC1 and PC2 explained about 75% of the
734 transcriptomic variance), one which contained the WT and the other contained only populations
735 that were more sensitive to oxidative stress than WT. One population that was as sensitive as WT
736 clustered independently, and two populations that clustered with the WT were more sensitive to
737 oxidative stress. Upon analysis of their gene hits, we found that they have loss-of-function
738 mutation in genes that relate to oxidative stress resistance.

739 To determine which genes and their expression differences may be responsible for the increased
740 oxidative stress sensitivity of most populations, we used the DESeq2 package to detect
741 differentially expressed genes between the two clusters (i.e. populations that are as sensitive and
742 more sensitive than WT)[129]. Gene functional categories and GO annotations were obtained from
743 Pombase data[40]. The RNA-seq analysis pipeline is available at
744 https://github.com/arnaud00013/Experimental_evolution_S_pombe.

745 **REFERENCES**

746 1. Kryazhimskiy, S., Rice, D. P., Jerison, E. R. & Desai, M. M. Microbial evolution. Global epistasis
747 makes adaptation predictable despite sequence-level stochasticity. *Science* **344**, 1519–1522
748 (2014).
749 2. Couce, A. & Tenaillon, O. A. The rule of declining adaptability in microbial evolution
750 experiments. *Front Genet* **6**, 99 (2015).
751 3. Johnson, M. S. *et al.* Phenotypic and molecular evolution across 10,000 generations in
752 laboratory budding yeast populations. *eLife* **10**, e63910 (2021).
753 4. Good, B. H., McDonald, M. J., Barrick, J. E., Lenski, R. E. & Desai, M. M. The dynamics of
754 molecular evolution over 60,000 generations. *Nature* **551**, 45–50 (2017).
755 5. Kinnersley, M. *et al.* Ex Uno Plures: Clonal Reinforcement Drives Evolution of a Simple
756 Microbial Community. *PLOS Genetics* **10**, e1004430 (2014).
757 6. Tenaillon, O. *et al.* Tempo and mode of genome evolution in a 50,000-generation experiment.
758 *Nature* **536**, 165–170 (2016).
759 7. Lang, G. I. *et al.* Pervasive genetic hitchhiking and clonal interference in forty evolving yeast
760 populations. *Nature* **500**, 571–574 (2013).
761 8. Venkataram, S. *et al.* Development of a Comprehensive Genotype-to-Fitness Map of
762 Adaptation-Driving Mutations in Yeast. *Cell* **166**, 1585-1596.e22 (2016).
763 9. Jerison, E. R. *et al.* Genetic variation in adaptability and pleiotropy in budding yeast. *eLife* **6**,
764 e27167.
765 10. Burke, M. K. *et al.* Genome-wide analysis of a long-term evolution experiment with Drosophila.
766 *Nature* **467**, 587–590 (2010).
767 11. Stroud, J. T. & Ratcliff, W. C. Long-term studies provide unique insights into evolution. *Nature*
768 **639**, 589–601 (2025).

769 12. Bakerlee, C. W., Ba, A. N. N., Shulgina, Y., Echenique, J. I. R. & Desai, M. M. Idiosyncratic
770 epistasis leads to global fitness-correlated trends. *Science* **376**, 630–635 (2022).
771 13. Echenique, J. I. R., Kryazhimskiy, S., Ba, A. N. N. & Desai, M. M. Modular epistasis and the
772 compensatory evolution of gene deletion mutants. *PLOS Genetics* **15**, e1007958 (2019).
773 14. Helsen, J. *et al.* Gene Loss Predictably Drives Evolutionary Adaptation. *Molecular Biology and*
774 *Evolution* **37**, 2989–3002 (2020).
775 15. Teng, X. *et al.* Genome-wide consequences of deleting any single gene. *Mol Cell* **52**, 485–494
776 (2013).
777 16. Galardini, M. *et al.* The impact of the genetic background on gene deletion phenotypes in
778 Saccharomyces cerevisiae. *Mol Syst Biol* **15**, e8831 (2019).
779 17. Blount, Z. D., Borland, C. Z. & Lenski, R. E. Historical contingency and the evolution of a key
780 innovation in an experimental population of Escherichia coli. *Proc Natl Acad Sci U S A* **105**,
781 7899–7906 (2008).
782 18. Huang, M.-E., Rio, A.-G., Nicolas, A. & Kolodner, R. D. A genomewide screen in Saccharomyces
783 cerevisiae for genes that suppress the accumulation of mutations. *Proceedings of the National*
784 *Academy of Sciences* **100**, 11529–11534 (2003).
785 19. Opulente, D. A. *et al.* Genomic factors shape carbon and nitrogen metabolic niche breadth
786 across Saccharomycotina yeasts. *Science* **384**, eadj4503 (2024).
787 20. Shen, X.-X. *et al.* Tempo and Mode of Genome Evolution in the Budding Yeast Subphylum. *Cell*
788 **175**, 1533-1545.e20 (2018).
789 21. Frost, A. *et al.* Comparing S. pombe and S. cerevisiae Genetic Interactions Reveals Functional
790 Repurposing and Identifies New Organelle Homeostasis and Mitosis Control Genes. *Cell* **149**,
791 1339–1352 (2012).

22. Rhind, N. *et al.* Comparative Functional Genomics of the Fission Yeasts. *Science* **332**, 930–936 (2011).
23. Forsburg, S. L. Overview of. *Current Protocols in Molecular Biology* **64**, 13.14.1-13.14.3 (2003).
24. Vyas, A., Freitas, A. V., Ralston, Z. A. & Tang, Z. Fission Yeast Schizosaccharomyces pombe: A Unicellular "Micromammal" Model Organism. *Curr Protoc* **1**, e151 (2021).
25. Ward, C. M. *et al.* Recombination, admixture and genome instability shape the genomic landscape of Saccharomyces cerevisiae derived from spontaneous grape ferments. *PLoS Genet* **20**, e1011223 (2024).
26. Peter, J. *et al.* Genome evolution across 1,011 Saccharomyces cerevisiae isolates. *Nature* **556**, 339–344 (2018).
27. Chen, V. *et al.* Evolution of haploid and diploid populations reveals common, strong, and variable pleiotropic effects in non-home environments. *eLife* **12**, e92899 (2023).
28. Shapira, R., Levy, T., Shaked, S., Fridman, E. & David, L. Extensive heterosis in growth of yeast hybrids is explained by a combination of genetic models. *Heredity (Edinb)* **113**, 316–326 (2014).
29. Shapira, R. & David, L. Genes with a Combination of Over-Dominant and Epistatic Effects Underlie Heterosis in Growth of Saccharomyces cerevisiae at High Temperature. *Front Genet* **7**, 72 (2016).
30. Conant, G. C. & Wolfe, K. H. Increased glycolytic flux as an outcome of whole-genome duplication in yeast. *Mol Syst Biol* **3**, 129 (2007).
31. Vowinckel, J. *et al.* The metabolic growth limitations of petite cells lacking the mitochondrial genome. *Nat Metab* **3**, 1521–1535 (2021).
32. Alam, S., Gu, Y., Reichert, P., Bähler, J. & Oliferenko, S. Optimization of energy production and central carbon metabolism in a non-respiring eukaryote. *Current Biology* **33**, 2175-2186.e5 (2023).

816 33. Chen, X. J. & Clark-Walker, G. D. The petite mutation in yeasts: 50 years on. *Int Rev Cytol* **194**,
817 197–238 (2000).
818 34. Dashko, S., Zhou, N., Compagno, C. & Piškur, J. Why, when, and how did yeast evolve alcoholic
819 fermentation? *FEMS Yeast Res* **14**, 826–832 (2014).
820 35. Kamrad, S. *et al.* Pyruvate kinase variant of fission yeast tunes carbon metabolism, cell
821 regulation, growth and stress resistance. *Mol Syst Biol* **16**, e9270 (2020).
822 36. Bergström, A. *et al.* A High-Definition View of Functional Genetic Variation from Natural Yeast
823 Genomes. *Molecular Biology and Evolution* **31**, 872–888 (2014).
824 37. Farlow, A. *et al.* The Spontaneous Mutation Rate in the Fission Yeast Schizosaccharomyces
825 pombe. *Genetics* **201**, 737–744 (2015).
826 38. Wood, V. *et al.* The genome sequence of Schizosaccharomyces pombe. *Nature* **415**, 871–880
827 (2002).
828 39. Blevins, W. R. *et al.* Uncovering de novo gene birth in yeast using deep transcriptomics. *Nat*
829 *Commun* **12**, 604 (2021).
830 40. Harris, M. A. *et al.* Fission stories: using PomBase to understand Schizosaccharomyces pombe
831 biology. *Genetics* **220**, iyab222 (2022).
832 41. Behringer, M. G. & Hall, D. W. Genome-Wide Estimates of Mutation Rates and Spectrum in
833 Schizosaccharomyces pombe Indicate CpG Sites are Highly Mutagenic Despite the Absence of
834 DNA Methylation. *G3 (Bethesda)* **6**, 149–160 (2015).
835 42. Schlackow, M. & Gullerova, M. Understanding non-coding DNA regions in yeast. *Biochemical*
836 *Society Transactions* **41**, 1654–1659 (2013).
837 43. Ohsawa, S. *et al.* Nitrogen signaling factor triggers a respiration-like gene expression program
838 in fission yeast. *The EMBO Journal* **43**, 4604–4624 (2024).

839 44. Vassiliadis, D., Wong, K. H., Andrianopoulos, A. & Monahan, B. J. A genome-wide analysis of
840 carbon catabolite repression in Schizosaccharomyces pombe. *BMC Genomics* **20**, 251 (2019).
841 45. Landolfo, S., Politi, H., Angelozzi, D. & Mannazzu, I. ROS accumulation and oxidative damage
842 to cell structures in *Saccharomyces cerevisiae* wine strains during fermentation of high-sugar-
843 containing medium. *Biochimica et Biophysica Acta (BBA) - General Subjects* **1780**, 892–898
844 (2008).
845 46. Synnott, J. M., Guida, A., Mulhern-Haughey, S., Higgins, D. G. & Butler, G. Regulation of the
846 Hypoxic Response in Candida albicans. *Eukaryot Cell* **9**, 1734–1746 (2010).
847 47. Koboldt, D. C. *et al.* VarScan 2: somatic mutation and copy number alteration discovery in
848 cancer by exome sequencing. *Genome Res* **22**, 568–76 (2012).
849 48. Koboldt, D. C. Best practices for variant calling in clinical sequencing. *Genome Medicine* **12**, 91
850 (2020).
851 49. Li, H. Toward better understanding of artifacts in variant calling from high-coverage samples.
852 *Bioinformatics* **30**, 2843–2851 (2014).
853 50. Zhu, Y. O., Siegal, M. L., Hall, D. W. & Petrov, D. A. Precise estimates of mutation rate and
854 spectrum in yeast. *Proceedings of the National Academy of Sciences of the United States of*
855 *America* **111**, E2310 (2014).
856 51. Lynch, M. *et al.* A genome-wide view of the spectrum of spontaneous mutations in yeast.
857 *Proceedings of the National Academy of Sciences of the United States of America* **105**, 9272
858 (2008).
859 52. Schacherer, J., Shapiro, J. A., Ruderfer, D. M. & Kruglyak, L. Comprehensive polymorphism
860 survey elucidates population structure of S. cerevisiae. *Nature* **458**, 342–345 (2009).
861 53. Gallone, B. *et al.* Origins, evolution, domestication and diversity of *Saccharomyces* beer
862 yeasts. *Current Opinion in Biotechnology* **49**, 148–155 (2018).

863 54. Duan, S.-F. *et al.* The origin and adaptive evolution of domesticated populations of yeast from
864 Far East Asia. *Nat Commun* **9**, 2690 (2018).
865 55. Chen, H., Blum, J. E., Thalacker-Mercer, A. & Gu, Z. Impact of the Whole Genome Duplication
866 Event on PYK Activity and Effects of a PYK1 Mutation on Metabolism in S. cerevisiae. *Front Mol*
867 *Biosci* **8**, 656461 (2021).
868 56. Frost, A. *et al.* Comparing S. pombe and S. cerevisiae Genetic Interactions Reveals Functional
869 Repurposing and Identifies New Organelle Homeostasis and Mitosis Control Genes. *Cell* **149**,
870 1339 (2012).
871 57. Aslett, M. & Wood, V. Gene Ontology annotation status of the fission yeast genome: preliminary
872 coverage approaches 100%. *Yeast* **23**, 913–919 (2006).
873 58. Khan, T., Douglas, G. M., Patel, P., Nguyen Ba, A. N. & Moses, A. M. Polymorphism Analysis
874 Reveals Reduced Negative Selection and Elevated Rate of Insertions and Deletions in
875 Intrinsically Disordered Protein Regions. *Genome Biology and Evolution* **7**, 1815–1826 (2015).
876 59. Dean, E. J., Davis, J. C., Davis, R. W. & Petrov, D. A. Pervasive and Persistent Redundancy
877 among Duplicated Genes in Yeast. *PLOS Genetics* **4**, e1000113 (2008).
878 60. Kim, D.-U. *et al.* Analysis of a genome-wide set of gene deletions in the fission yeast
879 Schizosaccharomyces pombe. *Nat Biotechnol* **28**, 617–623 (2010).
880 61. Dupré, S., Urban-Grimal, D. & Haguenauer-Tsapis, R. Ubiquitin and endocytic internalization in
881 yeast and animal cells. *Biochimica et Biophysica Acta (BBA) - Molecular Cell Research* **1695**,
882 89–111 (2004).
883 62. Zattas, D. & Hochstrasser, M. Ubiquitin-dependent Protein Degradation at the Yeast
884 Endoplasmic Reticulum and Nuclear Envelope. *Crit Rev Biochem Mol Biol* **50**, 1–17 (2015).
885 63. Lee, C.-Y. S., Yeh, T.-L., Hughes, B. T. & Espenshade, P. J. Regulation of the Sre1 hypoxic
886 transcription factor by oxygen-dependent control of DNA binding. *Mol Cell* **44**, 225–234 (2011).

887 64. Hughes, B. T. & Espenshade, P. J. Oxygen-regulated degradation of fission yeast SREBP by
888 Ofd1, a prolyl hydroxylase family member. *EMBO J* **27**, 1491–1501 (2008).
889 65. Porter, J. R., Lee, C.-Y. S., Espenshade, P. J. & Iglesias, P. A. Regulation of SREBP during hypoxia
890 requires Ofd1-mediated control of both DNA bindingand degradation. *Mol Biol Cell* **23**, 3764–
891 3774 (2012).
892 66. Matsuda, S., Kikkawa, U., Uda, H. & Nakashima, A. The S. pombe CDK5 ortholog Pef1 regulates
893 sexual differentiation through control of the TORC1 pathway and autophagy. *Journal of Cell*
894 *Science* **133**, jcs247817 (2020).
895 67. Todd, B. L., Stewart, E. V., Burg, J. S., Hughes, A. L. & Espenshade, P. J. Sterol Regulatory
896 Element Binding Protein Is a Principal Regulator of Anaerobic Gene Expression in Fission Yeast.
897 *Mol Cell Biol* **26**, 2817–2831 (2006).
898 68. Farrugia, G. & Balzan, R. Oxidative Stress and Programmed Cell Death in Yeast. *Front. Oncol.* **2**,
899 (2012).
900 69. Kaino, T., Tonoko, K., Mochizuki, S., Takashima, Y. & Kawamukai, M. Schizosaccharomyces
901 japonicus has low levels of CoQ10 synthesis, respiration deficiency, and efficient ethanol
902 production. *Bioscience, Biotechnology, and Biochemistry* **82**, 1031–1042 (2018).
903 70. Rodríguez-López, M. *et al.* Broad functional profiling of fission yeast proteins using phenomics
904 and machine learning. *eLife* **12**, RP88229 (2023).
905 71. Philpott, C. C., Leidgens, S. & Frey, A. G. Metabolic remodeling in iron-deficient fungi.
906 *Biochimica et Biophysica Acta (BBA) - Molecular Cell Research* **1823**, 1509–1520 (2012).
907 72. Rubio, A., Ghosh, S., Mülleder, M., Ralser, M. & Mata, J. Ribosome profiling reveals ribosome
908 stalling on tryptophan codons and ribosome queuing upon oxidative stress in fission yeast.
909 *Nucleic Acids Research* **49**, 383–399 (2021).

910 73. Kwon, E.-J. G. *et al.* Deciphering the Transcriptional-Regulatory Network of Flocculation in
911 Schizosaccharomyces pombe. *PLoS Genet* **8**, e1003104 (2012).
912 74. Stewart, G. G. Yeast Flocculation—Sedimentation and Flotation. *Fermentation* **4**, 28 (2018).
913 75. Dyson, H. J. & Wright, P. E. Intrinsically unstructured proteins and their functions. *Nat Rev Mol*
914 *Cell Biol* **6**, 197–208 (2005).
915 76. Chen, D. *et al.* Global Transcriptional Responses of Fission Yeast to Environmental Stress. *Mol*
916 *Biol Cell* **14**, 214–229 (2003).
917 77. Sawada, N., Ueno, S. & Takeda, K. Regulation of inorganic polyphosphate is required for proper
918 vacuolar proteolysis in fission yeast. *J Biol Chem* **297**, 100891 (2021).
919 78. Calvo, I. A., García, P., Ayté, J. & Hidalgo, E. The transcription factors Pap1 and Prr1 collaborate
920 to activate antioxidant, but not drug tolerance, genes in response to H2O2. *Nucleic Acids Res*
921 **40**, 4816–4824 (2012).
922 79. Quinn, J. *et al.* Two-Component Mediated Peroxide Sensing and Signal Transduction in Fission
923 Yeast. *Antioxidants & Redox Signaling* **15**, 153–165 (2011).
924 80. Leiter, É. *et al.* Protein phosphatase Z modulates oxidative stress response in fungi. *Fungal*
925 *Genet Biol* **49**, 708–716 (2012).
926 81. Semchyshyn, H. M., Abrat, O. B., Miedzobrodzki, J., Inoue, Y. & Lushchak, V. I. Acetate but not
927 propionate induces oxidative stress in bakers' yeast Saccharomyces cerevisiae. *Redox Rep* **16**,
928 15–23 (2013).
929 82. Pevala, V., Kolarov, J. & Polčic, P. Alterations in mitochondrial morphology
930 ofSchizosaccharomyces pombe induced by cell-death promoting agents. *Folia Microbiol* **52**,
931 381–390 (2007).
932 83. Chaves, S. R. *et al.* Regulation of Cell Death Induced by Acetic Acid in Yeasts. *Front Cell Dev*
933 *Biol* **9**, 642375 (2021).

934 84. Agus, H. H., Kok, G., Derinoz, E., Oncel, D. & Yilmaz, S. Involvement of Pca1 in ROS-mediated
935 apoptotic cell death induced by alpha-thujone in the fission yeast (Schizosaccharomyces
936 pombe). *FEMS Yeast Res* **20**, foaa022 (2020).
937 85. Guaragnella, N. & Bettiga, M. Acetic acid stress in budding yeast: From molecular mechanisms
938 to applications. *Yeast* **38**, 391–400 (2021).
939 86. Matsuo, Y. *et al.* Polypeptone Induces Dramatic Cell Lysis in ura4 Deletion Mutants of Fission
940 Yeast. *PLOS ONE* **8**, e59887 (2013).
941 87. Kosugi, M. *et al.* Stereochemical assignment of the unique electron acceptor 5'-
942 hydroxyphylloquinone, a polar analog of vitamin K1 in photosystem I. *Biosci Biotechnol*
943 *Biochem* **81**, 2244–2252 (2017).
944 88. Hughes, A. L., Todd, B. L. & Espenshade, P. J. SREBP pathway responds to sterols and
945 functions as an oxygen sensor in fission yeast. *Cell* **120**, 831–842 (2005).
946 89. Miki, R., Saiki, R., Ozoe, Y. & Kawamukai, M. Comparison of a coq7 deletion mutant with other
947 respiration-defective mutants in fission yeast. *The FEBS Journal* **275**, 5309–5324 (2008).
948 90. Pluskal, T., Sajiki, K., Becker, J., Takeda, K. & Yanagida, M. Diverse fission yeast genes required
949 for responding to oxidative and metal stress: Comparative analysis of glutathione-related and
950 other defense gene deletions. *Genes to Cells* **21**, 530–542 (2016).
951 91. Uchida, N. *et al.* Phenotypes of Fission Yeast Defective in Ubiquinone Production Due to
952 Disruption of the Gene for p-Hydroxybenzoate Polyprenyl Diphosphate Transferase. *J Bacteriol*
953 **182**, 6933–6939 (2000).
954 92. Wittkopp, P. J., Haerum, B. K. & Clark, A. G. Evolutionary changes in cis and trans gene
955 regulation. *Nature* **430**, 85–88 (2004).
956 93. Wittkopp, P. J. & Kalay, G. Cis-regulatory elements: molecular mechanisms and evolutionary
957 processes underlying divergence. *Nat Rev Genet* **13**, 59–69 (2011).

958 94. Liu, X., Li, Y. I. & Pritchard, J. K. Trans Effects on Gene Expression Can Drive Omnigenic
959 Inheritance. *Cell* **177**, 1022-1034.e6 (2019).
960 95. Yao, C. *et al.* Dynamic Role of trans Regulation of Gene Expression in Relation to Complex
961 Traits. *Am J Hum Genet* **100**, 571–580 (2017).
962 96. Renganaath, K. & Albert, F. W. Trans-eQTL hotspots shape complex traits by modulating
963 cellular states. *bioRxiv* 2023.11.14.567054 (2024) doi:10.1101/2023.11.14.567054.
964 97. Zakrzewska, A. *et al.* Genome-wide analysis of yeast stress survival and tolerance acquisition
965 to analyze the central trade-off between growth rate and cellular robustness. *Mol Biol Cell* **22**,
966 4435–4446 (2011).
967 98. Alejandro-Osorio, A. L. *et al.* The histone deacetylase Rpd3p is required for transient changes
968 in genomic expression in response to stress. *Genome Biol* **10**, R57 (2009).
969 99. Balcells, L. *et al.* The Pzh1 protein phosphatase and the Spm1 protein kinase are involved in the
970 regulation of the plasma membrane H+-ATPase in fission yeast. *FEBS Letters* **435**, 241–244
971 (1998).
972 100. Shahrouzi, P., Forouz, F., Mathelier, A., Kristensen, V. N. & Duijf, P. H. G. Copy number
973 alterations: a catastrophic orchestration of the breast cancer genome. *Trends in Molecular*
974 *Medicine* **30**, 750–764 (2024).
975 101. Al Tameemi, W., Dale, T. P., Al-Jumaily, R. M. K. & Forsyth, N. R. Hypoxia-Modified Cancer
976 Cell Metabolism. *Front. Cell Dev. Biol.* **7**, (2019).
977 102. Steele, C. D. *et al.* Signatures of copy number alterations in human cancer. *Nature* **606**,
978 984–991 (2022).
979 103. Denver, D. R., Morris, K., Lynch, M. & Thomas, W. K. High mutation rate and predominance
980 of insertions in the Caenorhabditis elegans nuclear genome. *Nature* **430**, 679–682 (2004).

981 104. Jensen, L. T. & Culotta, V. C. Regulation of *Saccharomyces cerevisiae FET4* by Oxygen and
982 Iron. *Journal of Molecular Biology* **318**, 251–260 (2002).
983 105. Daskalaki, I., Gkikas, I. & Tavernarakis, N. Hypoxia and Selective Autophagy in Cancer
984 Development and Therapy. *Front Cell Dev Biol* **6**, 104 (2018).
985 106. Slomka, S. *et al.* Experimental Evolution of Bacillus subtilis Reveals the Evolutionary
986 Dynamics of Horizontal Gene Transfer and Suggests Adaptive and Neutral Effects. *Genetics*
987 **216**, 543–558 (2020).
988 107. McDonald, M. J. Microbial Experimental Evolution - a proving ground for evolutionary theory
989 and a tool for discovery. *EMBO Rep* **20**, e46992 (2019).
990 108. Chaudhuri, B., Ingavale, S. & Bachhawat, A. K. Apd1(+), a Gene Required for Red Pigment
991 Formation in Ade6 Mutants of Schizosaccharomyces Pombe, Encodes an Enzyme Required for
992 Glutathione Biosynthesis: A Role for Glutathione and a Glutathione-Conjugate Pump. *Genetics*
993 **145**, 75–83 (1997).
994 109. Li, Y. *et al.* Hidden Complexity of Yeast Adaptation under Simple Evolutionary Conditions.
995 *Current Biology* **28**, 515-525.e6 (2018).
996 110. Williamson, T., Adiamah, D., Schwartz, J.-M. & Stateva, L. Exploring the genetic control of
997 glycolytic oscillations in Saccharomyces Cerevisiae. *BMC Systems Biology* **6**, 108 (2012).
998 111. Cytryńska, M., Frajnt, M. & Jakubowicz, T. Saccharomyces cerevisiae pyruvate kinase Pyk1
999 is PKA phosphorylation substrate in vitro. *FEMS Microbiology Letters* **203**, 223–227 (2001).
1000 112. Yu, Z.-Q. *et al.* Atg38-Atg8 interaction in fission yeast establishes a positive feedback loop
1001 to promote autophagy. *Autophagy* **16**, 2036–2051 (2020).
1002 113. Zhao, D. *et al.* Atg20- and Atg24-family proteins promote organelle autophagy in fission
1003 yeast. *J Cell Sci* **129**, 4289–4304 (2016).

1004 114. Su, Y., Chen, C., Huang, L., Yan, J. & Huang, Y. Schizosaccharomyces pombe Homologs of
1005 Human DJ-1 Are Stationary Phase-Associated Proteins That Are Involved in Autophagy and
1006 Oxidative Stress Resistance. *PLOS ONE* **10**, e0143888 (2015).
1007 115. Blanco, M. *et al.* An approach to the hypoxic and oxidative stress responses in
1008 Kluyveromyces lactis by analysis of mRNA levels. *FEMS Yeast Research* **7**, 702–714 (2007).
1009 116. Liu, J. & Barrientos, A. Transcriptional Regulation of Yeast Oxidative Phosphorylation
1010 Hypoxic Genes by Oxidative Stress. *Antioxidants & Redox Signaling* **19**, 1916–1927 (2013).
1011 117. Liu, J. & Wang, Z. Increased Oxidative Stress as a Selective Anticancer Therapy. *Oxid Med*
1012 *Cell Longev* **2015**, 294303 (2015).
1013 118. Mendoza, E. N., Ciriolo, M. R. & Ciccarone, F. Hypoxia-Induced Reactive Oxygen Species:
1014 Their Role in Cancer Resistance and Emerging Therapies to Overcome It. *Antioxidants* **14**, 94
1015 (2025).
1016 119. She, H. *et al.* Gene expression plasticity followed by genetic change during colonization a
1017 high-elevation environment. *eLife* **12**, (2023).
1018 120. Wahl, L. M. & Gerrish, P. J. The probability that beneficial mutations are lost in populations
1019 with periodic bottlenecks. *Evolution* **55**, 2606–2610 (2001).
1020 121. Sprouffske, K. & Wagner, A. Growthcurver: an R package for obtaining interpretable metrics
1021 from microbial growth curves. *BMC Bioinformatics* **17**, 172 (2016).
1022 122. Ritz, C., Baty, F., Streibig, J. C. & Gerhard, D. Dose-Response Analysis Using R. *PLOS ONE*
1023 **10**, e0146021 (2015).
1024 123. R Core Team. *R: A Language and Environment for Statistical Computing*. (R Foundation for
1025 Statistical Computing, Vienna, Austria, 2021).
1026 124. Oksanen, J. *et al. Vegan: Community Ecology Package*. (2025).

1027 125. Chen, S., Zhou, Y., Chen, Y. & Gu, J. fastp: an ultra-fast all-in-one FASTQ preprocessor.
1028 *Bioinformatics* **34**, i884–i890 (2018).
1029 126. Li, H. *et al*. The Sequence Alignment/Map format and SAMtools. *Bioinformatics* **25**, 2078–
1030 2079 (2009).
1031 127. Picard toolkit. *Broad Institute, GitHub repository* (2019).
1032 128. Liao, Y., Smyth, G. K. & Shi, W. featureCounts: an efficient general purpose program for
1033 assigning sequence reads to genomic features. *Bioinformatics* **30**, 923–930 (2014).
1034 129. Love, M. I., Huber, W. & Anders, S. Moderated estimation of fold change and dispersion for
1035 RNA-seq data with DESeq2. *Genome Biol* **15**, 550 (2014).
1036